ELSEVIER

Journal of Organometallic Chemistry 551 (1998) 313–330

Journal of Organometallic Chemistry

Complexes of gold(I) and platinum(II) with polyaromatic phosphine ligands [1]

Thomas E. Müller [a], Jennifer C. Green [b], D. Michael P. Mingos [a,*], C. Mary McPartlin [c], Conrad Whittingham [b], David J. Williams [a], Thomas M. Woodroffe [c]

[a] *Department of Chemistry, Imperial College of Science, Technology and Medicine, London SW7 2AY, UK*
[b] *Inorganic Chemistry Laboratories, University of Oxford, Oxford OX1 3QR, UK*
[c] *School of Applied Chemistry, University of North London, London N7 8DB, UK*

Received 17 June 1997

Abstract

Gold and platinum(II) complexes of the phosphine ligands PAr_nPh_{3-n} (Ar = naphthyl, anthracenyl, ferrocenyl and other polyaromatic groups) have been synthesised. The electron donating abilities of naphthyl and anthracenyl phosphine ligands has been explored using gas phase photoelectron spectral data on the parent phosphines and their relative complexing ability to platinum precursor molecules has been assessed by means of synthetic studies and NMR experiments. Their steric parameters have been estimated by the Tolman cone angle methodology using X-ray crystallographic data. The molecular structures of the gold complexes $[AuCl(PAn_2Ph)] \cdot CHCl_3$ and $[Au(PFc_2Ph)_2] \cdot CHCl_3$ have been determined. © 1998 Elsevier Science S.A.

Keywords: Gold; Platinum; Phosphine ligands

1. Introduction

The ability to fine-tune the steric and electronic properties of the ligands used in organometallic chemistry is a very important aspect of the subject. In order to investigate the effect of aromatic rings on the properties of phosphine ligands systematically, it was decided to synthesise a range of closely related polyaromatic phosphine ligands. Their properties were changed by varying the number of aromatic rings associated with the phosphines using naphthyl, anthracenyl, ferrocenyl and related substituents. These were chosen in part not only because of their differing steric requirements, but also because it has been recognised that the intramolecular phenyl interactions may contribute significantly to the total stability of phosphine stabilized metal clusters. It was also of interest to study the influence of these polyaromatic phosphines on the stabilities and structures of mononuclear transition metal compounds. Interestingly, these ligands, which are relatively easy to synthesise, have not been studied extensively previously either in mononuclear or polynuclear metal containing compounds [1] despite the fact that they closely resemble PPh_3.

Phosphine ligands, and particularly triphenylphosphine, have been widely used in organometallic chemistry to stabilise and solubilise complexes in low oxidation states [2]. The resultant complexes have shown a remarkable versatility. Indeed, a search of the Cambridge Crystallographic Structural Data Files [3] has established that no fewer than 3819 complexes containing triphenylphosphine have been structurally determined using X-ray crystallographic techniques. However, the polyaromatic ligands $PArPh_2$, PAr_2Ph, PAr_3 (Ar = anthracenyl (An), biphenyl (Bp), Ferrocenyl (Fc), 1-naphthyl (Np), 2-naphthyl (2Np) or phenanthrenyl (Pa)) have barely been studied.

Recently, we have described properties of gold complexes of polyaromatic phosphine ligands containing combinations of naphthyl and anthracenyl substituents [1]. Gold ethyne complexes have shown interesting properties [4] and

* Corresponding author.
[1] Dedicated to Professor Peter Maitlis on the occasion of his 65th birthday.

for example, have led to the definition of novel T-shaped hydrogen bonds between the proton of $CHCl_3$ and the triple bond in the chloroform solvates of gold ethyne complexes $R_3P–Au–C\equiv C–Au–PR_3 \cdot nCHCl_3$ ($PR_3 = PNpPh_2$, $n = 2$; $PR_3 = PNp_2Ph$, $n = 6$; $PR_3 = PFc_2Ph$, $n = 2$) [5], [6]. The synthesis and characterisation of the metal–metal bonded compounds of platinum $[Pt_2Cl_2(CO)_2(PR_3)_2]$ ($PR_3 = PNpPh_2$, PFc_2Ph) stabilised by these ligands have also been described [7]. In this paper, we investigate the changes within the series of anthracenyl and naphthyl phosphines when coordinated to gold and platinum. In order to obtain quantitative data on the steric requirements of these ligands the crystal structures of $[AuCl(PAn_2Ph)] \cdot CHCl_3$, (**1**) and $[Au(PFc_2Ph)_2]PF_6 \cdot CHCl_3$, (**2**) have been determined.

2. Results and discussion

2.1. Synthesis

The ligands $PArPh_2$, PAr_2Ph and PAr_3 (Ar = An and Np) and $PArPh_2$ (Ar = Bp, 2Np and Pa) were synthesised following literature procedures [8] from the appropriate chlorophosphine and the polyaromatic organo-lithium salt. To extend the range of available phosphines PFc_2Ph, which may be obtained commercially, was also studied. The biphenyl, naphthyl and phenanthrenyl containing ligands are virtually colourless, the anthracenyl containing ligands are yellow–orange crystalline solids and PFc_2Ph is orange. The ligands are air-stable as solids, but convert slowly in solution to the corresponding phosphine oxides.

2.2. Photoelectron spectra of the polyaromatic phosphines

In order to provide an indication of the relative donor properties of polyaromatic phosphines their gas phase photoelectron spectra were studied. Table 1 gives the ionisation energies of the molecular orbital which can most closely be associated with the lone-pair electrons of the phosphine. The energies decrease in the order PPh_3, $PNpPh_2$, PNp_2Ph to PNp_3, indicating that the phosphines become better donors as the number of naphthyl groups increases. No spectrum could be obtained for PAn_2Ph, but a comparison with the series of naphthyl phosphines shows that an anthracenyl group decreases the ionisation energy of the lone-pair electrons more than a naphthyl group. Again, a decrease in energy from PPh_3, $PAnPh_2$ to PAn_3 is observed. The introduction of a phenanthrenyl group has an even larger effect and the energy of the lone pair in $PPaPh_2$ is below the level for $PNpPh_2$ and $PAnPh_2$. A comparison of 1-naphthyl and 2-naphthyl diphenylphosphine shows that the point of attachment of the naphthyl group has little effect on the energy level of the lone-pair molecular orbital. Generally, it can be concluded that for these polyaromatic phosphines, the ionisation energy for the lone pair electrons decreases with the bulk of the substituent, making the phosphine electronically better donors, at least in the gas phase. This can be rationalised in terms of increased steric repulsion between the aromatic substituents which leads to an opening up of the angle Ar–P–Ar between the aromatic substituents. The molecular orbital which may be identified with the lone-pair has more p-orbital character as a consequence, and therefore lies at higher energies.

2.3. Gold(I) halide and nitrate complexes

The gold(I) complexes $[AuCl(PAr_nPh_{3-n})]$ were readily synthesised from $[AuCl(SMe_2)]$ and the appropriate phosphine (Yields $\gg$ 70%) and interconverted into the related nitrate salts $[Au(NO_3)(PAr_nPh_{3-n})]$ using $AgNO_3$ (Yields $\gg$ 50%). The compounds are stable crystalline solids and have the same colour as the parent phosphines. The chloro compounds are soluble in halogenated solvents, and the nitrate compounds are soluble in these solvents and also in THF. This series of compounds represents the first complete series of anthracenyl and naphthyl phosphine complexes and provide the first examples of PAn_2Ph and PAn_3 complexes.

Table 1
Phosphorus lone-pair ionisation energies IE/eV of the polyaromatic phosphines

PR_3	IE/eV	PR_3	IE/eV	PR_3	IE/eV	PR_3	IE/eV
PPh_3	7.81						
$PNpPh_2$	7.67	P_2NpPh_2	7.66	$PAnPh_2$	7.64	$PPaPh_2$	7.54
PNp_2Ph	7.50						
PNp_3	7.46			PAn_3	ca. 6.9		

Table 2
The measured $^{31}P\{^1H\}$ chemical shifts (ppm) of the polyaromatic phosphines, $[Au(NO_3)(PAr_nPh_{3-n})]$, $[AuCl(PAr_nPh_{3-n})]$ and of the phosphine oxides in comparison to the corresponding PPh_3 and PMe_3 compounds

	PR_3	OPR_3	$[AuCl(PR_3)]$	$[Au(NO_3)(PR_3)]$
$PAnPh_2$	−24.0	32.1	23.2	15.5
PAn_2Ph	−29.1	29.5	11.9	3.5
PAn_3	−44.0	40.5	−4.5	−13.0
$PBpPh_2$	−4.6	28.8	33.3	27.5
PFc_2Ph	−29.7	29.3	24.0	18.6
$PNpPh_2$	−13.6	33.5	26.9	20.0
PNp_2Ph	−22.8	37.0	17.4	8.7
PNp_3	−32.6	41.1	7.0	−3.4
PMe_3	−60.9	39.1	−9.7	−17.1
$PPaPh_2$	−12.1	33.4	26.7	20.9
PPh_3	−5.0	30.0	33.7	25.4

Table 2 summarises the $^{31}\{^1H\}$ chemical shifts of $[AuCl(PAr_nPh_{3-n})]$ and $[Au(NO_3)(PAr_nPh_{3-n})]$ with those for the free ligand and the phosphine oxide. The chemical shifts for the corresponding triphenylphosphine and trimethylphosphine compounds are given also for comparative purposes. Trends in the series of anthracenyl and naphthyl phosphine complexes have been discussed before [1] but the trends become less clear if all of the different phosphines are considered.

The proton NMR spectra of the polyaromatic phosphines show complex multiplets due to the aromatic systems between 8.8 and 7.0 ppm and PFc_2Ph shows additional signals between 4.5 and 4.2 ppm due to the ferrocenyl rings. For the anthracenyl and naphthyl phosphines, the signals could be assigned by performing a series of two dimensional ^1H-^1H-COSY experiments and by comparison of the spectra for different complexes. Data for the complexes $[AuCl(PAr_nPh_{3-n})]$ and $[Au(NO_3)(PAr_nPh_{3-n})]$ are given in Table 3 (Ar = Np) and Table 4 (Ar = An). The usual numbering for the anthracenyl group is shown in (1) and for the naphthyl group in (2), and the relevant assignments of the signals in the spectra are made on the basis of this numbering scheme.

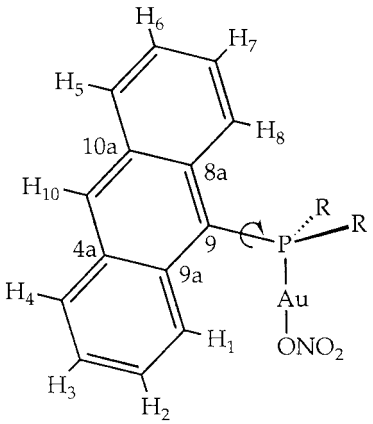

(1)

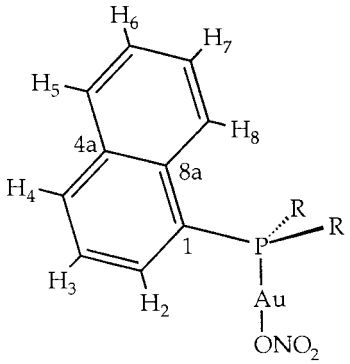

(2)

For the naphthyl phosphine complexes, the large shift of the signal for proton 8, and also for the protons 4 and 5 towards low field is noteworthy. The shift leaves these signals in an exposed position outside the phenyl region. The different complexes of each of these phosphines show slightly different positions for the protons 4, 5 and 8 which makes the signals for these protons useful indicators of the purity of the phosphine compounds. Similarly, in the anthracenyl complexes the signals for the proton 10 and the pairs of protons 1, 8 and 4, 5 show an even larger shift towards low-field and the signals can be used as purity indicators.

Once the proton signals were assigned, it was possible to assign the signals in the ^{13}C NMR spectra using ^{13}C–^1H-correlation experiments. The $^{13}C\{^1H\}$ NMR data for the tertiary carbon atoms in selected complexes of naphthyl and anthracenyl phosphines and their assignments are also given in Tables 3 and 4, respectively. There is no linear correlation between ^1H and ^{13}C chemical shifts. No NMR technique was available which could be used for an unambiguous assignment of the quaternary carbons and no attempt was made to assign the ^{13}C signals.

Table 3
Assignment of the ^{1}H NMR and selected ^{13}C{^{1}H} NMR signals for the complexes [AuCl(PNp_3)], (a); [Au(NO_3)(PNp_3)], (b); [AuCl(PNp_2Ph)], (c); [Au(NO_3)(PNp_2Ph)], (d); [AuCl($PNpPh_2$)], (e); [Au(NO_3)($PNpPh_2$)], (f)

	8	4	5	6	7	3	2	Phenyl
H NMR								
(a)	8.80d $^3J = 8.4$	8.08d $^3J = 7.6$	7.99d $^3J = 7.9$	7.60ddd $^3J = 7.9$ $^3J = 6.9$ $^4J = 1.0$	7.51ddd $^3J = 8.4$ $^3J = 6.9$ $^4J = 1.2$	7.30m	7.25m	
(b)	8.81d $^3J = 8.5$	8.15d $^3J = 8.0$	8.05d $^3J = 8.2$	7.64ddd $^3J = 8.2$ $^3J = 7.0$ $^4J = 0.8$	7.55ddd $^3J = 8.5$ $^3J = 7.0$ $^4J = 1.3$	7.36ddd $^3J = 8.0$ $^3J = 7.0$ $^4J_{HP} = 2.2$	7.30dd $^3J_{HP} = 15.3$ $^3J = 7.0$	
(c)	8.68d $^3J = 8.3$	8.05d $^3J = 7.9$	7.96d $^3J = 7.9$	7.68dd $^3J = 7.9$ $^3J = 6.0$	7.63 − 7.44m[a]	7.35ddd $^3J = 7.9$ $^3J = 6.9$ $^4J_{HP} = 2.0$	7.12ddd $^3J_{HP} = 14.5$ $^3J = 6.9$ $^4J = 1.2$	7.63 − 7.44m[a]
(d)	8.69d $^3J = 8.6$	8.10d $^3J = 8.1$	7.99d $^3J = 7.6$	7.74 − 7.52m[a]	7.74 − 7.52m[a]	7.38ddd $^3J = 8.1$ $^3J = 7.3$ $^4J_{HP} = 2.0$	7.13dd $^3J_{HP} = 14.9$ $^3J = 7.3$	7.74 − 7.52m[a]
(e)	8.41td $^3J = 8.5$ $^{4/5}J = 1.0$	8.04dd $^3J = 8.3$ $^4J = 1.2$	7.93ddd $^3J = 8.3$ $^{4/5}J = 1.6$	7.56m[a]	7.47m[a]	7.40ddd $^3J = 8.3$ $^3J = 7.2$ $^4J_{HP} = 2.0$	7.02ddd $^3J_{HP} = 14.5$ $^3J = 7.2$ $^4J = 1.2$	7.60ddd $^{\alpha}$ 7.56m[a] 7.47m[a]
(f)	8.42d $^3J = 8.3$	8.08d $^3J = 8.3$	7.96d $^3J = 7.9$	7.64 − 7.47m[a]	7.64 − 7.47m[a]	7.42ddd $^3J = 8.3$ $^3J = 7.4$ $^3J_{HP} = 2.0$	7.03dd $^3J_{HP} = 14.9$ $^3J = 7.4$	7.64 − 7.47m[a]
$^{13}C\{^1H\}$ NMR								
(b)	126.5d $^3J = 14.3$	134.3s	129.7s	127.4s	128.1s	125.6d $^3J = 12.9$	135.6d $^2J = 8.1$	
(c)	126.8d $^3J = 14.6$	134.0s	130.0s	127.7s	128.5s	125.7d $^3J = 12.2$	136.4d $^2J = 14.7$	134.8d β 133.2d γ 130.2d δ
(e)	126.3d $^3J = 14.7$	133.9d $^4J = 2.4$	129.9s	127.6s	128.4s	125.5d $^3J = 11.0$	135.4d $^2J = 13.4$	134.1d ϵ 132.8d ζ 130.0d η

[a] Denotes that the signals arise from naphthyl and phenyl protons and could not be assigned; chemical shifts are in ppm, coupling constants in Hertz; ^{1}H NMR: $J = J(^1H, ^1H)$, $J_{HP} = J(^1H, ^{31}P)$; ^{13}C NMR: $J = J(^{13}C, ^{31}P)$; $^{\alpha)}$ $^3J_{HP} = 13.5$, $^3J = 8.3$, $^4J = 1.4$, $^{\beta)}$ $J = 7.3$, $^{\gamma)}$ $J = 2.4$, $^{\delta)}$ $J = 12.2$, $^{\epsilon)}$ $J = 7.3$, $^{\zeta)}$ $J = 2.5$, $^{\eta)}$ $J = 12.2$.

2.4. Molecular structure of $[AuCl(PAn_2Ph)] \cdot CHCl_3$

To obtain the structural information needed for the determination of the Tolman cone angle of polyaromatic phosphines, an X-ray crystal structural analysis of the complex [AuCl(PAn_2Ph)] was performed. Suitable crystals were obtained from a chloroform solution of the compound. The compound crystallises in the space group $P2_1/n$ and includes one $CHCl_3$ molecule in the lattice. A perspective view of the molecule is shown in Fig. 1. The Au–P bond has a length of 2.250(2) Å and the Au–Cl bond of 2.281(2) Å. These compare well with the values for [AuCl(PPh_3)] [9] (2.235(3) Å, 2.279(3) Å, respectively), [AuCl(P^iPr_3)] [10] (2.239(2) Å, 2.284(3) Å, respectively) and [AuCl(PMe_3)] [10] (2.234(4) Å, 2.31(1) Å, respectively). In contrast to many other chloro-tertiary phosphine, gold(I) complexes where the P–Au–Cl unit is close to linearity (180° > P–Au–Cl > 177° for [AuCl(PR_3)], PR_3 = PPh_3 [9], PMe_3 [10], P^iPr_3 [10], $PTol_3$ [11]), the P–Au–Cl unit in [AuCl(PAn_2Ph)] deviates further from linearity with P–Au–Cl 173.9(1)°. The P–C bond lengths range from 1.821(6) Å to 1.843(6) Å and the Au–P–C angles are 119.1(2)° and 103.3(2)° for the anthracenyl substituents and 108.7(2)° for the phenyl group. The large difference of the Au–P–C angles for the three substituents probably reflects the steric crowding caused by the anthracene substituents. The

Table 4
Assignment of the ^{1}H NMR and selected ^{13}C{^{1}H} NMR signals for the complexes [AuCl(PAn$_3$)], (g); [Au(NO$_3$)(PAn$_3$)], (h); [AuCl(PAn$_2$Ph)], (i); [Au(NO$_3$)(PAn$_2$Ph)], (j); [AuCl(PAnPh$_2$)], (k); [Au(NO$_3$)(PAnPh$_2$)], (l) and [W(CO)$_5$(PAnPh$_2$)] [8], (m)

	10	1,8	4,5	3,6	2,7	Phenyl
H NMR[13]						
(g)	8.8s	8.4d $^3J = 8.9$	8.0d $^3J = 8.3$	7.3dd $^3J = 8.3$ $^3J = 6.6$	6.9dd $^3J = 8.9$ $^3J = 6.6$	
(h)	8.8s	8.3d $^3J = 8.8$	8.1d $^3J = 8.6$	7.3dd $^3J = 8.6$ $^3J = 6.4$	7.0dd $^3J = 8.8$ $^3J = 6.4$	
(i)	8.69b	8.23td $^3J = 9.1$ $^{4/5}J = 0.9$	8.01md $^3J = 8.4$ $^4J = 1.4$ $^4J = 1.2$ $^5J = 0.9$	7.35ddd $^3J = 8.4$ $^3J = 6.6$ $^4J = 0.9$	7.08ddd $^3J = 9.1$ $^3J = 6.6$ $^4J = 1.4$	8.07m 7.60m 7.47m
(j)	8.73s	8.25d $^3J = 9.1$	8.04d $^3J = 8.5$	7.39dd $^3J = 8.5$ $^3J = 6.3$	7.13dd $^3J = 9.1$ $^3J = 6.3$	7.99b 7.62tt$^{\alpha}$ 7.49ddd$^{\beta}$
(k)	8.73s	8.19d $^3J = 9.2$	8.06d $^3J = 8.6$	7.49 − 7.36m[a]	7.23mt $J = 7.6$	7.61mdd$^{\gamma}$ 7.49 − 7.36m[a]
(l)	8.77s	8.23d $^3J = 8.9$	8.09d $^3J = 8.6$	7.53 − 7.43m[a]	7.28mt $J = 6.8$	7.59ddd$^{\delta}$ 7.53 − 7.43m[a]
(m)	8.50s	7.66d $^3J = 9.1$	7.95d(m) $^3J = 8.5$	7.28ddd $^3J = 8.3$ $^3J = 6.6$ $J = 1$	7.01ddd $^3J = 9.1$ $^3J = 6.6$ $J = 1.4$	7.54dd 7.50dd 7.18 − 7.11m
C{^{1}H} NMR						
(h)	134.9d $^4J = 3.0$	125.2d $^3J = 14.8$	129.8s	125.5s	127.7s	
(i)	134.1d $^4J = 3.0$	125.2d $^3J = 14.6$	129.7s	125.4s	127.1s	135.4d$^{\epsilon}$ 129.8s 132.2s
(m)	132.0d	127.7d $J = 9.5$	129.6s	125.0s	124.9s	132.4d$^{\zeta}$ 129.7d$^{\eta}$ 128.8d$^{\theta}$

[a] Denotes that the signals arise from anthracenyl and phenyl protons and could not be assigned; chemical shifts are in ppm, coupling constants in Hz; ^{1}H NMR: $J = J(^1H, ^1H)$; ^{13}C NMR: $J = J(^{13}C, ^{31}P)$; $^{\alpha}$) $J = 7.5$, $J = 1.2$, $^{\beta}$) $J = 8.1$, $J = 7.5$, $J_{HP} = 2.5$, $^{\gamma}$) $J = 13.5$, $J = 7.9$, $^{\delta}$) $3J_{HP} = 13.9$, $^3J = 7.6$, $J = 2.0$, $^{\epsilon}$) $J = 15.1$, $^{\zeta}$) $J = 13.1$, $^{\eta}$) $J = 2.2$, $^{\theta}$) $J = 10.6$.

average Au–P–C angle is 110.7° which is significantly smaller than the average Au–P–C angle observed in [AuCl(PPh$_3$)] with 113.2°. The angles between the planes of the anthracenyl substituents and the corresponding Au–P–C$_{ipso}$ planes are 67.2° and 33.3°. The phenyl substituent is rotated by 25.2° against the Au–P–C$_{ipso}$ plane. In contrast to many gold(I) compounds which frequently exhibit short Au–Au intermolecular contacts, the gold atom in [AuCl(PAn$_2$Ph)] is linearly coordinated with no close approaches to the metal centre from other gold atoms. The steric bulk of the substituents probably rules out any close approaches of other molecules. The packing of the molecules is dominated by aromatic interactions between the anthracenyl groups. The solvate chloroform molecules loosely fill what would have otherwise been voids in the crystal lattice.

2.5. Molecular structure of [Au(PFc$_2$Ph)$_2$]PF$_6$ · CHCl$_3$

When Fc$_2$PhP–Au–C≡C–Au–PFc$_2$Ph [4] was reacted with [Cu(CH$_3$CN)$_4$]PF$_6$ several products resulted. One of the products was crystallised from CHCl$_3$–ethanol in orange cubes and was identified as [Au(PFc$_2$Ph)$_2$]PF$_6$ · CHCl$_3$ by means of an X-ray crystal structure analysis. The corresponding nitrate salt was prepared in 81% yield by reacting [Au(NO$_3$)(PFc$_2$Ph)] with one mol equivalent PFc$_2$Ph.

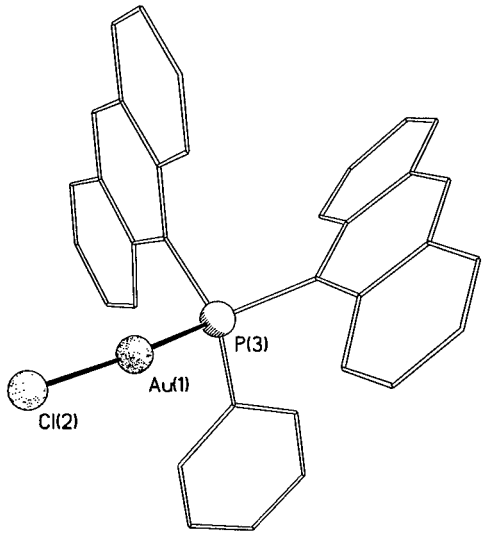

Fig. 1. Perspective view of the complex $[AuCl(PAn_2Ph)]\cdot CHCl_3$. Selected bond lengths (Å) and angles (°): Au(1)–P(3) = 2.250(2), Au(1)–Cl(2) = 2.281(2), P(3)–C(32) = 1.821(6), P(3)–C(4) = 1.832(6), P(3)–C(18) = 1.843(6), Cl(2)–Au(1)–P(3) = 173.9(1), Au(1)–P(3)–C(32) = 108.7(2), Au(1)–P(3)–C(4) = 119.1(2), Au(1)–P(3)–C(18) = 103.3(2).

The complex $[Au(PFc_2Ph)_2]PF_6\cdot CHCl_3$ (Fig. 2a,b) crystallises in the space group $P\bar{1}$, the symmetry centre relating two molecules in the unit cell. The Au–P bonds (2.295(5) and 2.296(5) Å) are significantly longer than the gold–phosphorus bond lengths of 2.234(2), 2.276(2) and 2.274(4) Å in $[AuCl(PFc_2Ph)]$ [12] $[Fc_2PhPAuC{\equiv}CAuPFc_2Ph]$ [4] and $[Fc_2PhPAuC{\equiv}CPh]$ [4], respectively, all being consistent with strong mutual *trans* influence of the diferrocenylphenylphosphine ligand. The angle P(1)–Au–P(2) is 169.3(2)° which is slightly distorted from the linear geometry observed in most Au(I) compounds. The P–C bond distances range from 1.77(1) Å to 1.82(1) Å. The Au–P–C angles for the ferrocenyl–C atoms are also significantly different from each other with angles, Au–P(1)–C(111) and Au–P(2)–C(311), of 108.0(3)° and 107.8(3)°, respectively, and very much smaller than angles, Au–P(1)–C(211) and Au–P(2)–C(411), of 119.1(3)° and 116.0(3)°, respectively. This large angular difference can be accounted for by the short intramolecular interactions between the ferrocenyl ring carbon atoms and the phenyl ring hydrogen atoms of H(2) · · · C(211) 3.160 Å, H(6) · · · C(111) 2.755 Å, H(8) · · · C(311) 2.790 Å and H(12) · · · C(421) 3.064 Å. Similar distortions of the Au–P–C angles occur in the monochloro complex $[AuCl(PFc_2Ph)]$ [12], with one relatively smaller Au–P–C(Fc) angle of 111.9(2)° with the other angle being larger, 118.3(2)°. The Au–P–C angles for the phenyl–C atoms, Au–P(1)–C(1) and Au–P(2)–C(7), are similar and equal to 111.8(4)° and 113.2(3)°.

The cyclopentadienyl rings within each ferrocenyl unit are not perfectly parallel with mean interplanar angles of 3.3° for Fc1 (defined by Fe(1) and C(111) to C(125)), 3.6° for Fc2 (Fe(2), C(211) to C(225)), 5.9° for Fc3 (Fe(3), C(311) to C(325)) and 4.4° for Fc4 (Fe(4), C(411) to C(425)). Each of the ferrocenyl moieties has an approximately eclipsed geometry with the following in-plane rotations of the ring with respect to each other: 8.8° for Fc1, 17.6° for Fc2, 5.9° for Fc3 and 16.5° for Fc4. The two substituent ferrocenyl units in each of the phosphines are oriented essentially orthogonal with respect to each other with a dihedral angle of 82.7° between the mean planes of C(111) to C(115) and C(211) to C(215) and 81.8° between the mean planes of C(311) to C(315) and C(411) to C(415). A similar orientation of the ferrocenyl groups has been observed for the parent phosphine PFc_2Ph [13]. The substituents in the phosphines are in a staggered conformation relative to the P–Au–P axis with the phenyl rings positioned *trans* to each other. Two of the ferrocenyl units (Fc1 and Fc3) are oriented approximately parallel with 163.5° between their molecular axes. The other two ferrocenyl units (Fc2 and Fc4) are oriented approximately perpendicular with respect to each other with 73.5° between their molecular axes.

2.6. Platinum complexes

In order to establish the relative complexing abilities of the ligands, the reactions of PNp_nPh_{3-n} ($n = 0$–3), $PAnPh_2$ and PAn_2Ph with $[PtCl_2(COD)]$, COD = cycloocta-1.5-diene, $[PtCl_2(CH_3CN)_2]$ and $[Pt(CH_3CN)_4](BF_4)_2$ were studied. The platinum compounds were dissolved in $CDCl_3$, CH_3NO_2 and CH_3CN, respectively. A solution with 2 mol equivalents of phosphine in $CDCl_3$ was added and a $^{31}P\{^1H\}$ NMR spectrum of the reaction mixture taken (Table 5).

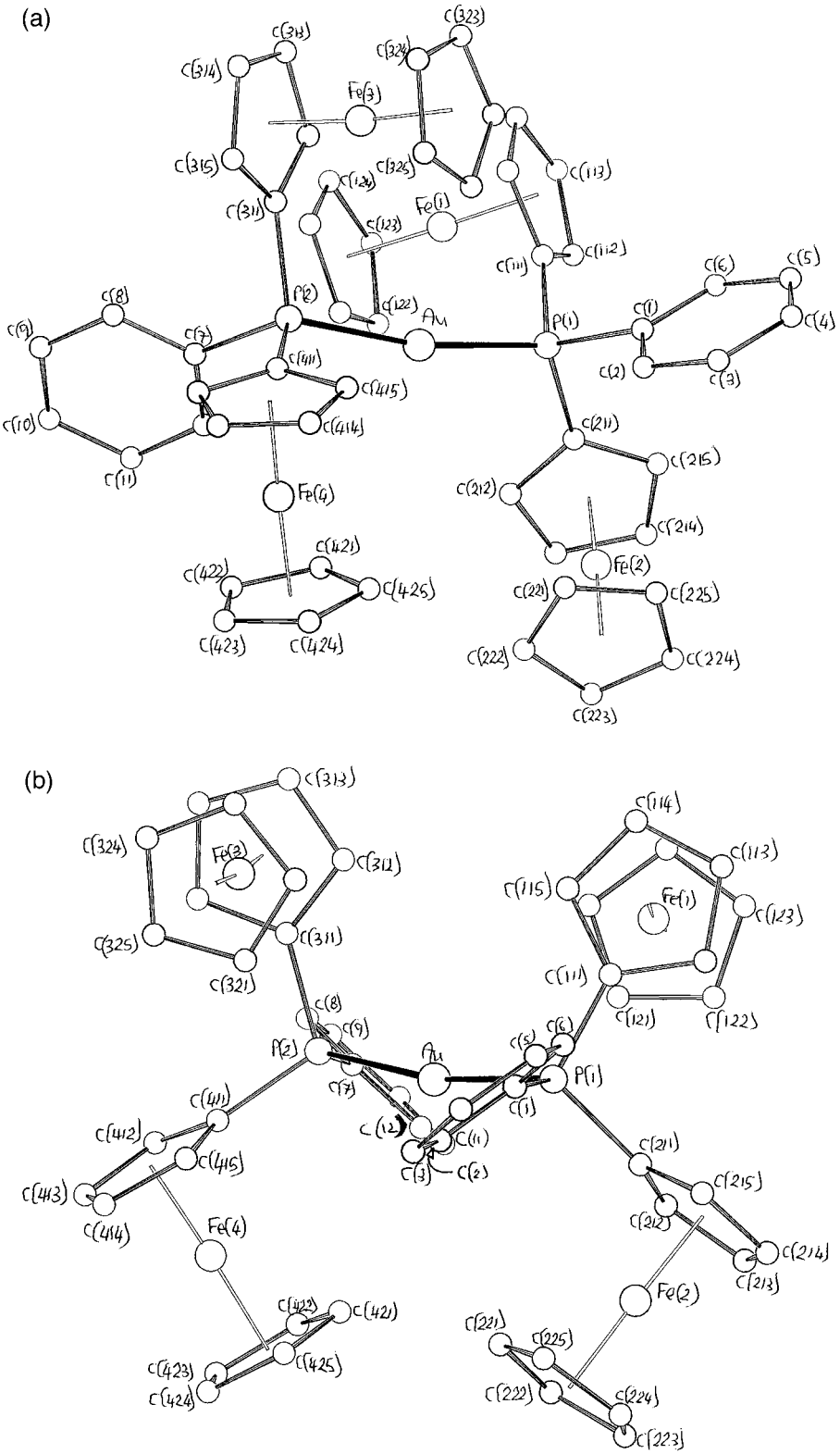

Fig. 2. (a) Top and (b) bottom: the molecular structure of $[Au(PFc_2Ph)_2]PF_6 \cdot CHCl_3$ showing the atomic labeling schemes. Selected bond lengths (Å) and angles (°): Au–P(1) = 2.295(5), Au–P(2) = 2.296(5), P(1)–C(311) = 1.80(1), P(2)–C(411) = 1.82(1), P(1)–Au–P(2) = 169.3(2), Au–P(1)–C(1) = 111.8(4), Au–P(1)–C(111) = 108.0(3), Au–P(1)–C(411) = 116.0(4); average distances (Å): Fe(1)–C = 2.049(8), Fe(2)–C = 2.049(8), Fe(3)–C = 2.044(8), Fe(4)–C = 2.046(8).

Table 5
$^{31}P\{^1H\}$ NMR of the reaction mixture of $[PtCl_2(COD)]$, $[PtCl_2(CH_3CN)_2]$ and $[Pt(CH_3CN)_4](BF_4)_2$ with two mol equivalents of the polyaromatic phosphines PNp_xPh_{3-x}, $PAnPh_2$ or PAn_2Ph

	$[PtCl_2(COD)]$		$[PtCl_2(CH_3CN)_2]$		$[Pt(CH_3CN)_4](BF_4)_2$	
Solvent	$CDCl_3$		CH_3NO_2–$CDCl_3$		CH_3CN–$CDCl_3$	
PR3	δ/ppm	$^1J(^{31}P, ^{195}Pt)$	δ/ppm	$^1J(^{31}P, ^{195}Pt)$	δ/ppm	$^1J(^{31}P, ^{195}Pt)$
$PNpPh_2$	10.3	3653 Hz	16.5	2600 Hz	13.5	2091 Hz
PNp_2Ph	(−)		11.9b, (−)	2319 Hz	11.4	2089 Hz
PNp_3 (−)	(−)		(−)		13.4	2104 Hz
					11.5	2119 Hz
$PAnPh_2$	(−)		10.9	2584 Hz	1.0	2061 Hz
PAn_2Ph	(−)		(−)		−3.0	2127 Hz

(−) denotes that a signal due to free phosphine is visible.

In the reaction mixture of $[PtCl_2(COD)]$ and $PNpPh_2$, a signal was visible at $\delta = 10.3$ ppm which was assigned to *cis*-$[PtCl_2(PNpPh_2)_2]$ on the basis of the large coupling constant $^1J(^{31}P, ^{195}Pt = 3653$ Hz which is typical *cis* coordinated phosphines [14]. Surprisingly, the reaction of $[PtCl_2(COD)]$ with the other phosphines initially showed only a signal due to free phosphine. After one day, the sample containing PNp_2Ph showed, besides a major signal for free phosphine, a small signal at $\delta = 18.3$ ppm which could be assigned to *trans*-$[PtCl_2(PNp_2Ph)_2]$ on the basis of the coupling constant $^1J(^{31}P, ^{195}Pt) = 2620$ Hz which is typical for *trans*-coordinated phosphines [14]. In the sample containing $PAnPh_2$, the signal due to the free phosphine had disappeared after one day. Several signals with Pt satellites were visible, but could not be unambiguously assigned.

The reaction of $[PtCl_2(CH_3CN)_2]$ with the polyaromatic phosphines showed that only $PNpPh_2$ and $PAnPh_2$ bind readily to the platinum compound. In the reaction mixture signals were visible at $\delta = 16.5$ ppm, $^1J(^{31}P, ^{195}Pt) = 2600$ ppm and $\delta = 10.9$ ppm, $^1J(^{31}P, ^{195}Pt) = 2584$ Hz, respectively. The corresponding compound started to precipitate after a few hours. The precipitates were filtered off after 2 days and were identified as *trans*-$[PtCl_2(PNpPh_2)_2]$ [15] and *trans*-$[PtCl_2(PAnPh_2)_2]$. The sample containing PNp_2Ph initially showed not only a broad signal at $\delta = 11.9$ ppm, $^1J(^{31}P, ^{195}Pt) = 2319$ Hz, but also a signal due to the free phosphine. After two days, both signals had disappeared and a signal at $\delta = 18.0$ ppm, $^1J(^{31}P, ^{195}Pt) = 2603$ Hz could be assigned to *trans*-$[PtCl_2(PNp_2Ph)_2]$. The phosphines PNp_3 and PAn_2Ph did not react with $[PtCl_2(CH_3CN)_2]$.

The compound $[Pt(CH_3CN)_4](BF_4)_2$ proved to be a much more reactive starting material. The phosphines $PNpPh_2$, PNp_2Ph, $PAnPh_2$ and PAn_2Ph reacted readily to form the compounds *trans*-$[Pt(CH_3CN)_2(PR_3)_2](BF_4)_2$. The reaction mixture with PNp_3 showed some free phosphine and two signals at $\delta = 13.4$ ppm, $^1J(^{31}P, ^{195}Pt) = 2104$ Hz and $\delta = 11.5$ ppm, $^1J(^{31}P, ^{195}Pt) = 2119$ Hz. The signal at 11.5 ppm could be assigned to *trans*-$[Pt(CH_3CN)_2(PNp_3)_2](BF_4)_2$ on the basis of the NMR spectrum of a sample from which the complex had been isolated and fully characterised. The signal at 13.4 ppm could not be assigned.

This series of experiments made it possible to place the phosphines into the following donor order in platinum(II) complexes:

$$PNpPh_2 > PAnPh_2 > PNp_2Ph > PAn_2Ph > PNp_3$$

$PNpPh_2$ is the only phosphine of the series to react readily with $[PtCl_2(COD)]$ to give *cis*-$[PtCl_2(PNpPh_2)_2]$. The phosphines $PNpPh_2$ and $PAnPh_2$ react readily with $[PtCl_2(CH_3CN)_2]$ to form *trans*-$[PtCl_2(PR_3)_2]$, while PNp_2Ph reacts slowly with this platinum precursor. All of the phosphines studied react with $[Pt(CH_3CN)_4](BF_4)_2$ to form $[Pt(CH_3CN)_2(PR_3)_2](BF_4)_2$. PNp_3 reacts more slowly with this platinum complex and a second product in the reaction mixture remains unidentified.

The observed reactivity series for naphthyl and anthracenyl phosphines is in marked contrast to PPh_3 which forms complexes much more readily. The complex *cis*-$[PtCl_2(PPh_3)_2]$ may be prepared from the reaction of $[PtCl_2(COD)]$ with PPh_3 [16,17]. The phosphorus NMR shows a signal at $\delta(^{31}P) = 15.5$ ppm, $^1J(^{31}P, ^{195}Pt) = 3679$ Hz. The corresponding *trans*-$[PtCl_2(PPh_3)_2]$ has a chemical shift of $\delta(^{31}P) = 19.8$ ppm, $^1J(^{31}P, ^{195}Pt) = 2637$ Hz. These values confirm the assignment of the $^{31}P\{^1H\}$ signals for the platinum complexes of polyaromatic phosphine ligands. The influence of steric factors on the rates of reaction of $[PtCl_2(COD)]$ with tertiary phosphines has been noted previously [18]. If $PMePh_2$ is used, *cis*-$[PtCl_2(PMePh_2)_2]$ results as the product. For PCy_3, the dimer $[Pt_2(\mu\text{-}Cl)_2Cl_2(PCy_3)_2]$ is proposed as the initial product, which is then cleaved further by PCy_3 to give *trans*-$[PtCl_2(PCy_3)_2]$. The phosphines $P(o\text{-}Tol)_3$ and $P(Mes)_3$ were found not to react with $[PtCl_2(COD)]$. Although olefin ligands are

Table 6
Calculated cone angles (°) for polyaromatic phosphines

Compound	Cone angle calculated
$[W(CO)_5(PAnPh_2)]$ [8]	156
$[Pd(dba)(PAnPh_2)_2]$ [R. Vilar, D.M.P. Mingos, unpublished results.]	164
$[NpPh_2P–Au–C\equiv C–Au–PNpPh_2]$ [4]	169
$[Np_2PhP–Au–C\equiv C–Au–PNp_2Ph]$ [4]	177
$[AuCl(PAn_2Ph)]$	186
PFc_2Ph [13]	190
$[Fc_2PhP–Au–C\equiv C–Au–PFc_2Ph]$ [4]	191
PAn_3 [8]	218

normally displaced by phosphorus(III) ligands the steric constraints associated with the larger polyaromatic phosphine ligands seem to prevent the nucleophilic attack of the phosphine on the diolefin complex.

2.7. Estimation of the steric requirement of polyaromatic phosphine ligands

Since only few structures of naphthyl and anthracenyl phosphine complexes have been described previously, it was of interest to use the structural data to compare the Tolman cone angles [19] of these ligands with those for the more widely studied triphenylphosphine [20,21]. The method used to determine the cone angle has been described previously [22]. Table 6 gives the values for the calculated cone angles for the naphthyl, anthracenyl and ferrocenyl substituted triphenylphosphine compounds.

The cone of $PAnPh_2$ depends on the orientation of the aromatic substituents on the phosphorus atom and on the metal to which the phosphine is coordinated [1]. Coordination to the early transition metal and tungsten, leads to a larger cone angle (164°) than coordination to the late transition metal palladium (156°). The cone angle of $PNpPh_2$ in $NpPh_2P–Au–C\equiv C–Au–PNpPh_2$ (169°) is larger than the cone angle of $PAnPh_2$ in the complexes given in Table 6. This is counter intuitive, but can be explained if one considers the conformation of the aromatic substituents [1]. The cone angle of the PNp_2Ph complex (177°) increases only slightly relatively to the cone angle in the $PNpPh_2$ complex, because the additional phenyl ring of the naphthyl group is able to tuck into empty space within the cone. The presence of two large anthracenyl groups leads to the large cone angle (186°) calculated for the complex $[AuCl(PAn_2Ph)]$. As the anthracenyl substituent is considerably larger than a naphthyl group a larger increase of the cone angle upon the introduction of the second polyaromatic substituent is expected. Thus an increase from 169° ($PNpPh_2$) to 177° (PNp_2Ph) is observed for the naphthyl phosphines, while a much larger increase from 156° or 164° ($PAnPh_2$) to 186° (PAn_2Ph) is observed for the anthracenyl phosphines. The introduction of two bulky ferrocenyl groups leads to an increase of the cone angle to 191°. This is probably due to the inability of this group to tuck into the space within the cone. The introduction of three anthracenyl groups in PAn_3 leads then to a further increase of the cone angle to 218°. The van der Waals surfaces of the anthracenyl groups touch each other so that the rotation around the PC bond is hindered. A variable temperature ^1H NMR experiment on $[Au(NO_3)(PAn_3)]$ has confirmed that in this complex the restricted rotation has a free energy of activation $\Delta G^{\#} = 51.0 \pm 1.1$ kJ mol^{-1} [1]. The phosphine molecule is very strained and therefore, it is not surprising that the synthesic route to this phosphine gives low yields [8].

The Tolman cone angles calculated for the polyaromatic phosphine ligands are much larger than of PPh_3 and increase in the order:

$$PAnPh_2 < PNpPh_2 < PNp_2Ph < PAn_2Ph < PFc_2Ph < PAn_3.$$

The smaller cone angle of $PAnPh_2$ relative to $PNpPh_2$ may be rationalised in terms of the conformations adopted by the aromatic substituents. Polyaromatic phosphines have the ability to adapt their steric requirement by adopting alternative ring conformations. In a statistical analysis of PPh_3 complexes, a cone angle of 148.2° with a large standard deviation of 4.9° has been calculated. The large spread of cone angles has highlighted the conformational variability of phosphines [22].

3. Conclusions

In order to investigate their steric and electronic properties, a series of closely related polyaromatic phosphine ligands was synthesised. The ionisation energy for the molecular orbital which can most closely be associated with the

lone pair of electrons of the phosphine was established by gas phase photoelectron spectroscopy. It decreases with the bulk of the substituent, and the larger phosphines are better electron donors.

Two complete series of complexes $[AuCl(PR_3)]$ and $[Au(NO_3)(PR_3)]$ with the chosen polyaromatic phosphines were synthesised. By a series of two dimensional NMR experiments and by comparative studies, it was possible to assign the ^1H and $^{13}C\{^1H\}$ NMR signals of the aromatic substituents. X-ray crystal structural determinations were performed on the gold complexes $[AuCl(PAn_2Ph)] \cdot CHCl_3$ and $[Au(PFc_2Ph)_2]PF_6 \cdot CHCl_3$.

The polyaromatic phosphine ligands showed the following relative complexing abilities towards platinum(II):

$$PNpPh_2 > PAnPh_2 > PNp_2Ph > PAn_2Ph > PNp_3.$$

This order does not follow the availability of the phosphorus lone-pair of electrons, but follows quite closely the order of the calculated cone angles, indicating that steric factors are the dominant influence in determining the reactivities of the polyaromatic phosphines towards platinum(II) and gold(I) centres.

4. Experimental

4.1. General

Standard Schlenk techniques and a nitrogen atmosphere was used routinely for carrying out the reactions, but no special precautions were taken to exclude oxygen during workup procedures, unless otherwise stated. Solvents were of reagent grade and used as purchased. For the syntheses of the complexes $[AuCl(PR_3)]$, $[Au(PR_3)_2]PF_6$, $[Pt(CH_3CN)_4](BF_4)_2$ and $[PtCl_2(CH_3CN)_2]$ the solvents were dried by published methods [23] and distilled under N_2.

4.2. Physical measurements and instrumentation

Infrared spectra were recorded on a Perkin–Elmer 1720 Infrared Fourier Transform Spectrometer as KBr pellets. Raman spectra were obtained on a Perkin–Elmer NIR FT-Raman 1700X Spectrometer equipped with a NdYAG-laser (1064 nm). ^1H, $^{31}P\{^1H\}$ and $^{13}C\{^1H\}$ NMR spectra were recorded on a JEOL JNM-EX270 and on Bruker WM-250, DRX-400 and AM-500 Fourier-transform NMR spectrometers with chemical shifts reported relative to TMS and H_3PO_4. For the $^{31}P\{^1H\}$ spectra, $PO(OMe)_3$ was used as internal reference using the conversion $\delta(PO(OMe)_3) = \delta(H_3PO_4) + 3.0$ ppm. The solid state ^1H and $^{13}C\{^1H\}$ NMR spectra were recorded on a Bruker MSL-300 Fourier-transform NMR spectrometer. Mass spectra were recorded on a VG AutoSpec-Q as FAB using 3-NBA as matrix. Crystallographic studies were performed on Imperial College [complex (**1**)] and on North London University [complex (**2**)]. Further details of the crystal studies are available from the director of the Cambridge Crystallographic Data Centre, 12 Union Road, Cambridge CB2 1EZ.

4.3. Synthesis of the phosphines

The phosphines were prepared following modified literature [8] methods, carefully excluding oxygen during all steps to minimise the oxidation to the corresponding phosphine oxides. Diferrocenylphenylphosphine was purchased from Aldrich.

4.4. PES-spectral measurements

The photoelectron spectra were recorded using a PES Laboratories 0078 spectrometer. Working pressures were 6–810 mbar; the phosphines were sublimed at 86°C (PPh_3), 135°C ($PNpPh_2$), 127°C ($P2NpPh_2$), 170°C (PNp_2Ph), ca. 250°C (PNp_3), 175°C ($PAnPh_2$), 218°C (PAn_3) and 137°C ($PPaPh_2$). Two sets of spectra were recorded for each sample using He(I) (21.22 eV) and He(II) (40.81 eV) radiation. The spectra were calibrated with He ^2S (ionised by the HeIIα radiation, KE = 16.23 eV), Xe$5^2P_{3/2}$ (IE = 12.13 eV), Xe $5^2P_{1/2}$ (IE = 13.44 eV) and N_2 ^2S (IE = 15.57 eV) calibration lines.

4.5. Synthesis of chloro(dimethylsulfide)gold(I)

A total of 5.066 g (25.7 mmol) of gold granules were suspended in a mixture of 25 cm^3 DMSO and 50 cm^3 $HCl_{conc}(aq)$ and stirred at 95°C (reflux condenser, open to air) for several hours until most of the gold had dissolved. The mixture was kept in the freezer overnight and the solid consisting of white crystals, a yellow powder and

undissolved gold was filtered off. The solid was extracted with MeOH, the white crystals dissolved in CH_2Cl_2 and the remaining gold (0.613 g, 3.1 mmol) recovered. The CH_2Cl_2 solution was mixed with hexane and the volume reduced until a white precipitate formed which was filtered off and dried in vacuo to yield 5.737 g [$AuCl(SMe_2)$]. The MeOH solution was reduced slowly to a small volume, the crystals which formed were filtered off, washed with Et_2O and $CHCl_3$, recrystallised from MeOH–Bu_2O and dried in vacuo to yield yellow crystals (1.218 g) which were characterised to be $HAuCl_4 \cdot 2Me_2SO$.

4.5.1. [$AuCl(SMe_2)$]

Yield: 5.737 g, 86% (relative to Au). Found: C, 8.1; H, 1.8%. Calc. for C_2H_6AuClS: C, 8.1; H, 2.0%. ^{1}H NMR ($CDCl_3$): δ 2.8 (s). $\tilde{\nu}_{max}$ cm^{-1} 1437s, 1423s, 1414s, 1384w, 1034s, 995s, 345m, 326m.

4.5.2. [$HAuCl_4$] · $2Me_2SO$

Yield: 1.218 g, 11% (relative to Au). Found: C, 9.9; H, 2.6; Au, 35.4; Cl, 25.1%. Calc. for $C_4H_{13}AuCl_4S_2O_2$: C, 9.7; H, 2.6; Au, 39.7; Cl, 28.6%. ^{1}H NMR (D_2O): δ 2.5 (s). ^{13}C{^{1}H} NMR (D_2O): δ 40.8 (s). ^{13}C NMR (CD_3OD): δ 39.3 (q, ^1J(^{13}C, ^{1}H) 138 Hz). ^{1}H MAS ECHO: δ 3.0 (s), 16.4 (s). ^{13}C{^{1}H} MAS: δ 41.0 (s). $\tilde{\nu}_{max}$ cm^{-1} 3000m, 2915m, 1423m (S–CH_3), 1325m δ(S–CH_3), 1181b, vs ν(S=O), 1027m, 939m, 907m, 717b, vs, 353vs ν(Au–Cl), 323w. Raman: 3008w, 2921m, 691w, 345vs ν(Au–Cl), 321s (Au–Cl).

4.6. Synthesis of the chloro(tertiary-phosphine)gold(I) complexes

About 1.0 mmol of phosphine was dissolved in CH_2Cl_2 (20 cm^3) and added over a period of 5 min to a magnetically-stirred solution of [$AuCl(SMe_2)$] (0.295 g, 1.0 mmol) in CH_2Cl_2 (20 cm^3). The complex was precipitated by addition of hexane, followed by removal of dimethylsulfide and CH_2Cl_2 in a partial vacuum. The product was filtered off, recrystallised from CH_2Cl_2–hexane and dried in vacuo.

4.6.1. [$AuCl(PNp_3)$]

Yield: 91%. Found: C, 51.1; H, 2.9%. Calc. for $C_{30}H_{21}AuClP$: C, 51.0; H, 3.2%. ^{31}P{^{1}H} NMR ($CDCl_3$): δ 7.0 (s). ^{1}H NMR ($CDCl_3$): δ 8.80 (d, ^3J(^{1}H, ^{1}H) 8.4 Hz, 3 H), 8.08 (d, ^3J(^{1}H, ^{1}H) 7.6 Hz, 3H), 7.99 (d, ^3J(^{1}H, ^{1}H) 7.9 Hz, 3H), 7.60 (ddd, ^3J(^{1}H, ^{1}H) 7.9, ^3J(^{1}H, ^{1}H) 6.9, ^4J(^{1}H, ^{1}H) 1.0 Hz, 3H), 7.51 (ddd, ^3J(^{1}H, ^{1}H) 8.4, ^3J(^{1}H, ^{1}H) 6.9, ^4J(^{1}H, ^{1}H) 1.2 Hz, 3H), 7.30 (m, 3H), 7.25 (m, 3H). $\tilde{\nu}_{max}$ cm^{-1} 337 ν(AuCl).

4.6.2. [$AuCl(PNp_2Ph)$]

Yield: 97%. Found: C, 51.4; H, 3.2%. Calc. for $C_{26}H_{19}AuClP$: C, 52.5; H, 3.2%. ^{31}P{^{1}H} NMR ($CDCl_3$): δ 17.4 (s). ^{13}C{^{1}H} NMR ($CDCl_3$): δ 136.4 (d, J(^{1}H, ^{31}P) 14.7 Hz), 134.8 (d, J(^{1}H, ^{31}P) 7.3 Hz), 134.0 (s), 133.2 (d, J(^{1}H, ^{31}P) 2.4 Hz), 130.2 (d, J(^{1}H, ^{31}P) 12.2 Hz), 130.0 (s), 128.5 (s), 127.7 (s), 126.8 (d, J(^{1}H, ^{31}P) 14.6 Hz), 125.7 (d, J(^{1}H, ^{31}P) 12.2 Hz), 124.3 (d, J(^{1}H, ^{31}P) 61 Hz). ^{1}H NMR ($CDCl_3$): δ 8.68 (d, ^3J(^{1}H, ^{1}H) 8.3 Hz, 2H), 8.05 (d, ^3J(^{1}H, ^{1}H) 7.9 Hz, 2H), 7.96 (d, ^3J(^{1}H, ^{1}H) 7.9 Hz, 2H), 7.68 (dd, ^3J(^{1}H, ^{1}H) 7.9, ^3J(^{1}H, ^{1}H) 6.0 Hz, 2H), 7.63 − 7.44 (m, 7H), 7.35 (ddd, ^3J(^{1}H, ^{1}H) 7.9, ^3J(^{1}H, ^{1}H) 6.9, ^4J(^{1}H, ^{31}P) 2.0 Hz, 2H), 7.12 (ddd, ^3J(^{1}H, ^{31}P) 14.5, ^3J(^{1}H, ^{1}H) 6.9, ^4J(^{1}H, ^{1}H) 1.2 Hz, 2H). $\tilde{\nu}_{max}$ cm^{-1} 331 ν(AuCl). m/z 594 (M^+), 559 ($M–Cl^-$).

4.6.3. [$AuCl(PNpPh_2)$]

Yield: 86%. Found: C, 48.3; H, 2.8%. Calc. for $C_{22}H_{17}AuClP$: C, 48.5; H, 3.1%. ^{31}P{^{1}H} NMR ($CDCl_3$): 26.9 (s). ^{13}C{^{1}H} NMR ($CDCl_3$): δ 135.4 (d, J(^{1}H, ^{31}P) 13.4 Hz), 134.4 (d, J(^{1}H, ^{31}P) 8.5 Hz), 134.1 (d, J(^{1}H, ^{31}P) 7.3 Hz), 133.9 (d, J(^{1}H, ^{31}P) 2.4 Hz), 133.5 (d, J(^{1}H, ^{31}P) 12.2 Hz), 132.8 (d, J(^{1}H, ^{31}P) 2.5 Hz), 130.0 (d, J(^{1}H, ^{31}P) 12.2 Hz), 129.9 (s), 128.7 (d, J(^{1}H, ^{31}P) 63.5 Hz), 128.4 (s), 127.6 (s), 126.3 (d, J(^{1}H, ^{31}P) 14.7 Hz), 125.5 (d, J(^{1}H, ^{31}P) 11.0 Hz), 125.1 (d, J(^{1}H, ^{31}P) 61.0 Hz). ^{1}H NMR, resolution enhanced, ($CDCl_3$): δ 8.41 (td, ^3J(^{1}H, ^{1}H) 8.5, $^{4/5}J$(^{1}H, ^{1}H) 1.0 Hz, 1H), 8.04 (dd, ^3J(^{1}H, ^{1}H) 8.3, ^4J(^{1}H, ^{1}H) 1.2 Hz, 1H), 7.93 (d, ^3J(^{1}H, ^{1}H) 8.2, ^4J(^{1}H, ^{1}H) 1.6 Hz, 1H), 7.60 (ddd, ^3J(^{1}H, ^{31}P) 13.5, ^3J(^{1}H, ^{1}H) 8.3, ^4J(^{1}H, ^{1}H) 1.4 Hz, 4H), 7.56 (m, 3H), 7.47 (m, 5H), 7.40 (ddd, ^3J(^{1}H, ^{1}H) 8.3, ^3J(^{1}H, ^{1}H) 7.2, ^4J(^{1}H, ^{31}P) 2.0 Hz, 1H), 7.02 (ddd, ^3J(^{1}H, ^{31}P) 14.5, ^3J(^{1}H, ^{1}H) 7.2, ^4J(^{1}H, ^{1}H) 1.2 Hz, 1H). $\tilde{\nu}_{max}$ cm^{-1} 327 ν(AuCl). m/z 1053 (M^+ + $AuPNpPh_2$), 544 (M^+), 509 ($M–Cl^-$).

4.6.4. [$AuCl(PAn_3)$]

Yield: 72%. ^{31}P{^{1}H} NMR ($CDCl_3$): δ −4.5 (s). ^{13}C{^{1}H} NMR ($CDCl_3$): 134.4 − 122.0 (s). ^{1}H NMR ($CDCl_3$): δ 8.8 (s, 3H), 8.4 (d, ^3J(^{1}H, ^{1}H) 8.9 Hz, 6H), 8.0 (d, ^3J(^{1}H, ^{1}H) 8.3 Hz, 6H), 7.3 (dd, ^3J(^{1}H, ^{1}H) 8.3 Hz, ^3J(^{1}H, ^{1}H) 6.6 Hz, 6H), 6.9 (dd, ^3J(^{1}H, ^{1}H) 8.9 Hz, ^3J(^{1}H, ^{1}H) 6.6 Hz, 6H). $\tilde{\nu}_{max}$ cm^{-1} 327 ν(AuCl). m/z 794 (M^+), 759 ($M–Cl^-$).

4.6.5. [AuCl(PAn$_2$Ph)]

Yield: 93%. Found: C, 56.2; H, 3.4%. Calc. for 0.5 CH_2Cl_2 solvent molecule, $C_{34.5}H_{24}AuCl_2P$: C, 56.2 H, 3.2%. $^{31}P\{^1H\}$ NMR ($CDCl_3$): δ 12.0 (s). $^{13}C\{^1H\}$ NMR ($CDCl_3$): δ 135.4 (d, $J(^1H, ^{31}P)$ 15.1 Hz), 134.1 (d, $J(^1H, ^{31}P)$ 3.0 Hz), 133.6 (d, $J(^1H, ^{31}P)$ 8.3 Hz), 132.2 (s), 131.6 (d, $J(^1H, ^{31}P)$ 58.6 Hz), 131.4 (d, $J(^1H, ^{31}P)$ 9.1 Hz), 129.8 (s), 129.7 (s), 127.1 (s), 125.4 (s), 125.2 (d, $J(^1H, ^{31}P)$ 14.6 Hz), 120.9 (d, $J(^1H, ^{31}P)$ 55.3 Hz). ^1H NMR, resolution enhanced, ($CDCl_3$): δ 8.69 (b), 8.23 (td, $^3J(^1H, ^1H)$ 9.1, $^{4/5}J(^1H, ^1H)$ 0.9 Hz). 8.07 (m), 8.01 (md, $^3J(^1H, ^1H)$ 8.4 Hz, $^4J(^1H, ^1H)$ 1.4, $^4J(^1H, ^1H)$ 1.2, $^5J(^1H, ^1H)$ 0.9 Hz), 7.60 (m), 7.47 (m), 7.35 (ddd, $^3J(^1H, ^1H)$ 8.4, $^3J(^1H, ^1H)$ 6.6, $^4J(^1H, ^1H)$ 0.9 Hz), 7.08 (ddd, $^3J(^1H, ^1H)$ 9.1, $^3J(^1H, ^1H)$ 6.6, $^4J(^1H, ^1H)$ 1.4 Hz). $\tilde{\nu}_{max}$ cm^{-1} 328s (AuCl).

*4.6.6. Crystal structure determination of [AuCl(PAn$_2$Ph)] · CHCl$_3$, (**1**)*

Crystal data for (**1**): $C_{35}H_{24}AuCl_4P$, $M = 814.28$, monoclinic, $a = 9.8833(12)$ Å, $b = 16.558(2)$ Å, $c = 19.383(4)$ Å, $\beta = 104.587(11)°$, $U = 3069.8(7)$ Å^3, space group $P2_1/n$, $Z = 4$, $D_c = 1.762$ g cm^{-3}, $F(000) = 1584$, yellow block, crystal dimensions: $0.40 \times 0.29 \times 0.15$ mm, the crystal was coated in araldite to prevent desolvation, $\mu(Mo–K_\alpha) = 52.17$ cm^{-1}.

Data collection and refinement: Siemens P4/PC diffractometer, scans using graphite monochromated Mo–K_α radiation. 5703 reflections were collected of which 5373 were unique and 4075 were observed ($2.1° \leq 2\theta \leq 25.0°$, $I > 2\sigma(I)$). The structure was solved by direct methods. Full matrix anisotropic refinement of all non hydrogen atoms based on F^2 produced $R_1 = 0.0388$ and $wR_2 = 0.0866$ using absorption corrected data. All calculations were performed using the SHELXTL software package [24]. Atom coordinates are listed in Table 7.

4.6.7. [AuCl(PAnPh$_2$)]

Yield: 91%. Found: C, 51.8; H, 2.9%. Calc. for $C_{26}H_{19}AuClP$: C, 52.5; H, 3.2%. $^{31}P\{^1H\}$ NMR ($CDCl_3$): δ 23.2 (s). ^1H NMR ($CDCl_3$): δ 8.73 (s, 1H), 8.19 (d, $^3J(^1H, ^1H)$ 9.2 Hz, 2H). 8.06 (d, $^3J(^1H, ^1H)$ 8.6 Hz, 2H). 7.61 (mdd, $^3J(^1H, ^{31}P)$ 13.5, $^3J(^1H, ^1H)$ 7.9 Hz, 4H), 7.49 − 7.36 (m, 8H), 7.23 (mt, $^3J(^1H, ^1H)$ 7.6, 2H). $\tilde{\nu}_{max}$ cm^{-1} 331 ν(AuCl). m/z 594 (M^+), 559 ($M–Cl^-$).

4.6.8. [AuCl(PBpPh$_2$)]

Yield: 77%. Found: C, 50.2; H, 3.3%. Calc. for $C_{24}H_{19}AuClP$: C, 50.5; H, 3.3%. $^{31}P\{^1H\}$ NMR ($CDCl_3$): δ 33.3 (s). ^1H NMR ($CDCl_3$): δ 7.36–7.72 (m). IR: 329 cm^{-1} ν(AuCl).

4.6.9. [AuCl(PPaPh$_2$]

Yield: 90%. Found: C, 52.2; H, 3.1%. Calc. for $C_{26}H_{19}AuClP$: C, 52.5; H, 3.2%. $^{31}P\{^1H\}$ NMR ($CDCl_3$): δ 26.7 (s). ^1H NMR ($CDCl_3$): 8.8 − 7.3 (m). $\tilde{\nu}_{max}$ cm^{-1} 326 ν(AuCl).

4.6.10. [AuCl(PPh$_3$]

Yield: 93%. Found: C, 43.5; H, 2.9%. Calc. for $C_{18}H_{15}AuClP$: C, 43.7; H, 3.0%. $^{31}P\{^1H\}$ NMR ($CDCl_3$): δ 33.7 (s). ^1H NMR ($CDCl_3$): δ 7.55 − 7.45 (m). m/z 494 (M^+), 459 ($M–Cl^-$).

4.6.11. [AuCl(PFc$_2$Ph)]

Yield: 99%. Found: C, 43.7; H, 3.1%. Calc. for $C_{26}H_{23}AuClFe_2P$: C, 43.9; H, 3.2%. $^{31}P\{^1H\}$ NMR ($CDCl_3$): δ 24.0 (s). ^1H NMR ($CDCl_3$): δ 7.8 (m, 2H), 7.5 (m, 3H), 4.5 (m, 6H), 4.2 (m, 12H). $\tilde{\nu}_{max}$ cm^{-1} 329 cm^{-1}, ν(AuCl). m/z 710 (M^+).

4.6.12. [AuCl(PMe$_3$)]

Yield: 97%. Found: C, 11.7; H, 2.6%. Calc. for C_3H_9AuClP: C, 11.7; H, 2.9%. $^{31}P\{^1H\}$ NMR ($CDCl_3$): δ-9.7 (s). ^1H NMR ($CDCl_3$): δ 1.6 (m, $^2J(^1H, ^{31}P)$ 11 Hz). $\tilde{\nu}_{max}$ cm^{-1} 312 ν(AuCl). m/z 273 ($M–Cl^-$).

4.7. Synthesis of the tertiary-phosphinegold(I)nitrate complexes

Silver nitrate (0.170 g, 1.0 mmol) was dissolved in MeOH (5 cm^3) and added to a magnetically stirred solution of 1.0 mmol chloro(tertiary-phosphine)gold(I) in CH_2Cl_2 (50 cm^3). The solution was stirred in the dark for 1 h. The solution was then filtered and the complex precipitated by addition of hexane, followed by removal of dichloromethane in a partial vacuum. The product was filtered off, recrystallised from CH_2Cl_2–hexane and dried in vacuo.

4.7.1. [Au(NO3)(PNp$_3$)]

Yield: 93%. Found: C, 49.0; H, 2.8; N, 1.9%. Calc. for one CH_2Cl_2 solvent molecule, $C_{31}H_{23}AuCl_2NO_3P$: C, 49.2; H, 3.0; N,1.9%. $^{31}P\{^1H\}$ NMR (CD_2Cl_2): δ −3.4 (br s). $^{13}C\{^1H\}$ NMR ($CDCl_3$): δ 135.6 (d, $^4J(^1H, ^{31}P)$ 8.1

Table 7
Atomic coordinates and equivalent isotropic displacement coefficients (Å^2) for [AuCl(PAn$_2$Ph)] · CHCl$_3$

Atom	x	y	z	$U_{(eq)}^a$
Au(1)	0.17140(3)	0.19430(2)	0.393977(13)	0.03651(9)
Cl(2)	0.2566(2)	0.12086(12)	0.31465(10)	0.0577(5)
P(3)	0.0684(2)	0.25727(10)	0.47014(8)	0.0314(4)
C(4)	0.1778(6)	0.3092(4)	0.5478(3)	0.0316(13)
C(5)	0.3111(7)	0.3377(4)	0.5456(4)	0.0365(15)
C(6)	0.3526(8)	0.3534(4)	0.4808(4)	0.048(2)
C(7)	0.4837(10)	0.3820(5)	0.4839(5)	0.067(2)
C(8)	0.5812(9)	0.3956(5)	0.5482(6)	0.075(3)
C(9)	0.5479(8)	0.3831(5)	0.6097(5)	0.065(2)
C(10)	0.4128(7)	0.3553(4)	0.6115(4)	0.044(2)
C(11)	0.3750(8)	0.3478(4)	0.6752(4)	0.048(2)
C(12)	0.2392(7)	0.3299(4)	0.6777(4)	0.039(2)
C(13)	0.1947(9)	0.3315(4)	0.7427(4)	0.050(2)
C(14)	0.0645(10)	0.3199(5)	0.7446(4)	0.064(2)
C(15)	−0.0406(9)	0.3066(5)	0.6802(4)	0.058(2)
C(16)	−0.0046(7)	0.3019(4)	0.6175(4)	0.041(2)
C(17)	0.1355(7)	0.3120(4)	0.6125(3)	0.0386(15)
C(18)	−0.0122(7)	0.1738(3)	0.5085(3)	0.0317(14)
C(19)	0.0849(7)	0.1195(4)	0.5522(3)	0.0316(14)
C(20)	0.2335(7)	0.1254(4)	0.5643(3)	0.0368(15)
C(21)	0.3224(8)	0.0723(5)	0.6066(4)	0.049(2)
C(22)	0.2719(8)	0.0071(5)	0.6401(4)	0.053(2)
C(23)	0.1319(9)	−0.0022(5)	0.6292(4)	0.053(2)
C(24)	0.0353(7)	0.0524(4)	0.5853(3)	0.038(2)
C(25)	−0.1081(8)	0.0412(4)	0.5746(4)	0.047(2)
C(26)	−0.2034(7)	0.0919(4)	0.5323(3)	0.041(2)
C(27)	−0.3503(8)	0.0768(5)	0.5216(4)	0.054(2)
C(28)	−0.4468(8)	0.1249(5)	0.4804(4)	0.056(2)
C(29)	−0.4017(7)	0.1907(5)	0.4454(4)	0.051(2)
C(30)	−0.2644(7)	0.2071(4)	0.4536(4)	0.043(2)
C(31)	−0.1576(6)	0.1591(4)	0.4970(3)	0.0323(14)
C(32)	−0.0508(7)	0.3335(4)	0.4212(3)	0.0349(15)
C(33)	−0.0872(8)	0.4008(4)	0.4526(4)	0.051(2)
C(34)	−0.1770(9)	0.4572(5)	0.4126(5)	0.070(3)
C(35)	−0.2298(9)	0.4461(5)	0.3418(5)	0.068(3)
C(36)	−0.1938(9)	0.3787(6)	0.3081(5)	0.066(2)
C(37)	−0.1033(8)	0.3236(4)	0.3469(4)	0.049(2)
C(40)	0.2699(11)	−0.0856(8)	0.2602(6)	0.100(4)
Cl(41)	0.3522(4)	−0.1753(2)	0.2898(3)	0.1398(15)
Cl(42)	0.0908(4)	−0.0984(3)	0.2250(2)	0.153(2)
Cl(43)	0.3459(4)	−0.0389(2)	0.1984(2)	0.1191(11)

[a] Equivalent isotropic U defined as one third of the trace of the orthogonalized U_{ij} tensor.

Hz, CH), 134.6 (d, $J(^1H, ^{31}P)$ 8.6 Hz, C), 134.3 (s, CH), 134.1 (d, $J(^1H, ^{31}P)$ 11.4 Hz, C),129.7 (s, CH), 128.1 (s, CH), 127.4 (s, CH), 126.5 (d, $^3J(^1H, ^{31}P)$ 14.3 Hz, CH), 125.6 (d, $^3J(^1H, ^{31}P)$ 12.9 Hz, CH), 121.5 (d, $^1J(^1H, ^{31}P)$ 67.3 Hz, C). ^{1}H NMR (CD_2Cl_2): δ 8.81 (d, 3H, $^3J(^1H, ^1H)$ 8.5 Hz), 8.15 (d, 3H, $^3J(^1H, ^1H)$ 8.0 Hz), 8.05 (d, 3H, $^3J(^1H, ^1H)$ 8.2 Hz), 7.64 (ddd, 3H, $^3J(^1H, ^1H)$ 8.2, $^3J(^1H, ^1H)$ 7.0, $^4J(^1H, ^1H)$ 0.8 Hz), 7.55 (ddd, 3H, $^3J(^1H, ^1H)$ 8.5, $^3J(^1H, ^1H)$ 7.0, $^4J(^1H, ^1H)$ 1.3 Hz), 7.36 (ddd, 3H, $^3J(^1H, ^1H)$ 8.0, $^3J(^1H, ^1H)$ 7.0, $^4J(^1H, ^{31}P)$ 2.2 Hz), 7.30 (dd, br, 3H, $^3J(^1H, ^{31}P)$ 15.3, $^3J(^1H, ^1H)$ 7.0 Hz). $\tilde{\nu}_{max}$ cm^{-1} 1500, 1277 $\nu(NO_3^-)$. m/z 609 (M–NO_3^-).

4.7.2. [Au(NO$_3$)(PNp$_2$Ph)]

Yield: 79%. Found: C, 49.2; H, 2.9; N,2.0%. Calc. for $C_{26}H_{19}AuNO_3P$: C, 50.2; H, 3.1; N, 2.2%. $^{31}P\{^1H$ NMR ($CDCl_3$): δ 8.7 (s). ^{1}H NMR ($CDCl_3$): δ 8.69 (d, $^3J(^1H, ^1H)$ 8.6 Hz, 2H), 8.10 (d, $^3J(^1H, ^1H)$ 8.1 Hz, 2H), 7.99 (d, $^3J(^1H, ^1H)$ 7.6 Hz, 2H), 7.74 − 7.52 (m, 9H), 7.38 (ddd, $^3J(^1H, ^1H)$ 8.1, $^3J(^1H, ^1H)$ 7.3, $^4J(^1H, ^{31}P)$ 2.0 Hz, 2H), 7.13 (dd, $^3J(^1H, ^{31}P)$ 14.9, $^3J(^1H, ^1H)$ 7.3 Hz, 2H). $\tilde{\nu}_{max}$ cm^{-1} 1499, 1272 $\nu(NO_3^-)$. m/z 559 (M–NO_3^-).

4.7.3. [Au(NO$_3$)(PNpPh$_2$)]

Yield: 43%. Found: C, 45.8; H, 2.7; N, 2.4%. Calc. for $C_{22}H_{17}AuNO_3P$: C, 46.2; H, 3.0; N, 2.5%. $_{31}P\{^1H\}$ NMR ($CDCl_3$): δ 20.0 (s). ^{1}H NMR ($CDCl_3$): δ 8.42 (d, $^3J(^1H, ^1H)$ 8.3 Hz, 1H), 8.08 (d, $^3J(^1H, ^1H)$ 8.3 Hz, 1H), 7.96 (d,

$^3J(^1H, ^1H)$ 7.9 Hz, 1H), 7.64 − 7.47 (m, 12H), 7.42 (ddd, $^3J(^1H, ^1H)$ 8.3, $^3J(^1H, ^1H)$ 7.4, $^4J(^1H, ^{31}P)$ 0.7 Hz, 1H). 7.03 (dd, $^3J(^1H, ^{31}P)$ 14.9, $^3J(^1H, ^1H)$ 7.4 Hz, 1H). $\tilde{\nu}_{max}$ cm^{-1} 1498, 1272 $\nu(NO_3^-)$.

4.7.4. [Au(NO$_3$)(PAn$_3$)]

Yield: 53%. Found: C, 61.1; H, 3.0; N, 1.6%. Calc. for $C_{42}H_{27}AuNO_3P$: C, 61.4; H, 3.3; N, 1.7%. $^{31}P\{^1H\}$ NMR ($CDCl_3$): δ-13.0 (s). $^{13}C\{^1H\}$ NMR ($CDCl_3$): δ 134.9 (d, $^4J(^1H, ^{31}P)$ 3.0 Hz, CH), 134.3 (br s, C), 131.4 (d, $J(^{13}C, ^{31}P)$ 9.7 Hz, C), 129.8 (s, CH), 127.7 (s, CH), 125.5 (s, CH), 125.2 (d, $^3J(^{13}C, ^{31}P)$ 14.8 Hz, CH), 121.3 (d, $^1J(^{13}C, ^{31}P)$ 55.9 Hz, C). ^1H NMR ($CDCl_3$): δ 8.8 (s, 3H), 8.3 (d, $^3J(^1H, ^1H)$ 8.8 Hz, 6H), 8.1 (d, $^3J(^1H, ^1H)$ 8.6 Hz, 6H), 7.3 (dd, $^3J(^1H, ^1H)$ 8.6, $^3J(^1H, ^1H)$ 6.4 Hz, 6H), 7.0 (dd, $^3J(^1H, ^1H)$ 8.8, $^3J(^1H, ^1H)$ 6.4 Hz, 6H). $\tilde{\nu}_{max}$ cm^{-1} 1513, 1270 $\nu(NO_3^-)$. *m/z* 759 ($M–NO_3^-$).

4.7.5. [Au(NO$_3$)(PAn$_2$Ph)]

Yield: 79%. Found: C, 56.5; H, 3.3; N, 1.7%. Calc. for $C_{34}H_{23}AuNO_3P$: C, 56.7; H, 3.2; N, 1.9%. $^{31}P\{^1H\}$ NMR ($CDCl_3$): δ 3.5 (s). ^1H NMR ($CDCl_3$): δ 8.73 (s, 2H), 8.25 (d, $^3J(^1H, ^1H)$ 9.1 Hz, 4H), 8.04 (d, $^3J(^1H, ^1H)$ 8.5 Hz, 4H), 7.99 (b, 2H), 7.62 (tt, $^3J(^1H, ^1H)$ 7.5, $^4J(^1H, ^1H)$ 1.2 Hz, 1H), 7.49 (ddd, $^3J(^1H, ^1H)$ 8.1, $^3J(^1H, ^1H)$ 7.5, $^4J(^1H, ^{31}P)$ 2.5 Hz, 2H), 7.39 (dd, $^3J(^1H, ^1H)$ 8.5, $^3J(^1H, ^1H)$ 6.3 Hz, 4H), 7.13 (dd, $^3J(^1H, ^1H)$ 9.1, $^3J(^1H, ^1H)$ 6.3 Hz, 4H). *m/z* 659 ($M–NO_3$).

4.7.6. [Au(NO$_3$)(PAnPh$_2$)]

Yield: 95%. Found: C, 49.7; H, 3.2; N, 2.0%. Calc. for $C_{26}H_{19}AuNO_3P$: C, 49.9; H, 3.0; N, 2.2%. $^{31}P\{^1H$ NMR ($CDCl_3$): δ 15.5 (s). ^1H NMR ($CDCl_3$): δ 8.77 (s, 1H), 8.23 (d, $^3J(^1H, ^1H)$ 8.9 Hz, 2H), 8.09 (d, $^3J(^1H, ^1H)$ 8.6 Hz, 2H), 7.59 (ddd, $^3J(^1H, ^1H)$ 13.9, $^3J(^1H, ^1H)$ 7.6, $J(^1H, ^1H)$ 2.0 Hz, 4H), 7.53 − 7.43 (m, 8H), 7.28 (mt, $^3J(^1H, ^1H)$ 6.8 Hz, 2H). $\tilde{\nu}_{max}$ cm^{-1} 1496, 1268 $\nu(NO_3^-)$. *m/z* 921 ($M–NO_3^- + PAnPh_2$), 559 ($M–NO_3^-$).

4.7.7. [Au(NO$_3$)(PPh$_3$)]

Yield: 66%. Found: C, 41.4; H, 2.9; N, 2.5%. Calc. for $C_{18}H_{15}AuNO_3P$: C, 41.5; H, 2.9; N, 2.7%. $^{31}P\{^1H\}$ NMR ($CDCl_3$): δ 25.4 (s). ^1H NMR ($CDCl_3$): δ 7.59 − 7.48 (m). *m/z* 459 ($M–NO_3^-$).

4.7.8. [Au(NO$_3$)(PBpPh$_2$)]

Yield: 97%. Found: C, 48.1; H, 2.8; N, 2.2%. Calc. for $C_{24}H_{19}AuNO_3P$: C, 48.2; H, 3.2; N, 2.4%. $^{31}P\{^1H\}$ NMR ($CDCl_3$): δ 27.5 (s). ^1H NMR ($CDCl_3$): δ 7.3–7.7 (m). $\tilde{\nu}_{max}$ cm^{-1} 1503, 1276 $\nu(NO_3^-)$.

4.7.9. [Au(NO$_3$)(PPaPh$_2$)]

Yield: 90%. Found: C, 46.4; H, 2.6; N, 2.4%. Calc. for one CH_2Cl_2 solvent molecule, $C_{27}H_{21}AuCl_2NO_3P$: C, 46.0; H, 3.0; N, 2.0%. $^{31}P\{^1H\}$ NMR ($CDCl_3$): δ 20.9 (s). ^1H NMR ($CDCl_3$): δ 8.8 − 7.3 (m). $\tilde{\nu}_{max}$ cm^{-1} 1510, 1263 $\nu(NO_3^-)$. *m/z* 559 ($M–NO_3^-$).

4.7.10. [Au(NO$_3$)(PFc$_2$Ph)]

Yield: 94%. Found: C, 42.1; H, 2.7; N, 1.7%. Calc. for $C_{26}H_{23}AuFe_2NO_3P$: C, 42.3; H, 3.1; N, 1.9%. $^{31}P\{^1H\}$ NMR ($CDCl_3$): δ 18.6 (s). ^1H NMR ($CDCl_3$): δ 7.8 (m, 2H), 7.5 (m, 3H), 4.5 (m, 6H), 4.2 (m, 12H). $\tilde{\nu}_{max}$ cm^{-1} 1490, 1273 $\nu(NO_3^-)$. *m/z* 737 (M^+), 675 ($M–NO_3^-$).

4.7.11. [Au(NO$_3$)(PMe$_3$)]

Yield: 96%. Found: C, 11.4; H, 2.4; N, 4.1%. Calc. for $C_3H_9AuNO_3P$: C, 10.7; H, 2.7; N, 4.2%. $^{31}P\{^1H\}$ NMR ($CDCl_3$): δ-17.1 (s). ^1H NMR ($CDCl_3$): δ 1.7 (d, $^2J(^1H, ^{31}P)$ 12 Hz). $\tilde{\nu}_{max}$ cm^{-1} 1487, 1271 $\nu(NO_3^-)$. *m/z* 426 ($M–NO_3^- + 2PMe_3$), 349 ($M–NO_3^- + PMe_3$), 273 ($M–NO_3^-$).

4.8. Synthesis of bis(tertiary-phosphine)gold(I) complexes

4.8.1. [Au(PFc$_2$Ph)$_2$]PF$_6$ · CHCl$_3$

[$Fc_2PhP–Au–C≡C–Au–PFc_2Ph$] [4] (0.20 g, 0.15 mmol) was dissolved in THF and a solution of $[Cu(CH_3CN)_4]PF_6$ (0.207 g, 0.43 mmol) in CH_3CN added. Et_2O was added and the precipitate formed filtered off. Heptane was added and the solvent removed until a precipitate developed. The product was filtered off, washed with hexane and dried in vacuo. Large orange crystals were obtained by layering a $CHCl_3$ solution of the product with EtOH. $^{31}P\{^1H\}$ NMR ($CDCl_3$): δ 37.4 (s).

4.8.2. Crystal structure determination of [Au(PFc$_2$Ph)$_2$]PF$_6$ · CHCl$_3$, (2)

Crystal data for (**2**): $C_{53}H_{47}AuCl_3F_6Fe_4P_3$, $M = 1417.55$, triclinic, space group P, $a = 11.571(3)$ Å, $b = 23.423(5)$ Å, $c = 10.252(3)$ Å, $\alpha = 94.38(2)°$, $\beta = 107.33(2)°$, $\gamma = 99.28(2)°$, $U = 2595(1)$ Å^3, $Z = 2$, $D_c = 1.82$ g cm^{-3}, μ(Mo–K$_\alpha$) = 40.8 cm^{-1}, $\lambda = 0.71069$ Å, $F(000) = 1396$, orange plate, crystal dimensions: 0.50 × 0.48 × 0.43 mm.

Data collection: data were collected on a Philips PW1100 four-circle diffractometer using the method described previously [25], with graphite monochromated Mo–K$_\alpha$ radiation and a scan width of 0.80° and a scan speed of 0.05° s^{-1}. A total of 5972 reflections, in the range of $6° \leq 2\theta \leq 42°$, were scanned, giving 3321 unique data with $I/\sigma(I) \geq 3.0$.

Structure solution and refinement [26]: the coordinates of the gold atom and the two phosphorus atoms bonded to it were deduced from a Patterson synthesis. The remaining non-hydrogen atoms were located from subsequent Fourier and difference-Fourier synthesis maps. The hydrogen atoms of the phenyl rings and the chloroform solvate molecule were included into the structure calculations at calculated positions (C–H, 0.96 Å) and only one common thermal parameter was refined (to a value of 0.08603 Å^2). The low quality diffraction exhibited by the crystal may be attributed to the disorder about the PF_{6-} counter-ion and the chloroform solvate molecule; the fluorine and chlorine atoms occurred at two alternative sites with assigned population parameters of 0.5 corresponding to a random distribution of two orientations of these symmetrical species throughout the crystal. Empirical absorbtion corrections [27] (max = 1.17, min = 0.88) were applied after initial refinement with isotropic thermal parameters for all atoms. Anisotropic thermal parameters were assigned to all non-hydrogen atoms except the fluorine, chloroform and the carbon atoms of the substituted cyclopentadiene rings. Full-matrix least-squares refinement converged at R and R_w values of 0.0576 and 0.0562, respectively, with weighing schemes of $1/[\sigma^2(F_o)]$ applied to the individual reflections. Atom coordinates are listed in Table 8.

4.8.3. [Au(PFc$_2$Ph)$_2$]NO$_3$

[Au(NO$_3$)(PFc$_2$Ph)] (0.320 g, 0.43 mmol was dissolved in CH_2Cl_2 and a solution of PFc$_2$Ph (0.207 g, 0.43 mmol) in CH_2Cl_2 added. Hexane was added and the solvent removed until a precipitate developed. The product was filtered off, recrystallised from CH_2Cl_2–Et_2O and from CH_2Cl_2–EtOH and dried in vacuo.

Yield: 0.427 g, 81%. Found: C,50.8; H,3.6; N,1.0%. Calc. for $C_{52}H_{46}AuFe_4NO_3P2$: C, 50.3; H, 4.1; N, 1.0%. ^{1}H NMR ($CDCl_3$): δ 7.9 (m, 2H), 7.7 (m, 3H), 4.8 (s, 2H), 4.7 (s, 2H), 4.6 (s, 2H), 4.4 (s, 2H), 4.2 (s, 10H). ^{31}P{^{1}H} NMR ($CDCl_3$): δ 37.4 (s). m/z 1153 (M–NO$_3$).

4.9. Synthesis of platinum precursors

4.9.1. [PtCl$_2$(CH$_3$CN)$_2$] [28]

Platinum dichloride (2.95 g = 11.1 mmol) was suspended in CH_3CN (150 cm^3), the mixture refluxed for 4 h and filtered hot. The solution was reduced to a small volume on a rotary evaporator and the compound precipitated with Et_2O. The solid was filtered off, washed with Et_2O and dried in vacuo.

Yield: 3.80 g, 99%. Found: C, 14.0; H, 1.6; N, 8.1%. Calc. for $C_4H_6Cl_2N_2Pt$: C, 13.8; H, 1.7; N, 8.0%. ^{1}H NMR (CD_3CN): δ 2.3 (t, ^4J(^{1}H, ^{195}Pt) 11 Hz). ^{13}C{^{1}H} NMR (CD_3NO_2): δ 118.5 (s), 3.6 (s). $\tilde{\nu}_{max}$ cm^{-1} 2970s, 2922s, 2332s (C≡N), 2306m (C≡N), 1409s, 1355m, 1030s, 432w, 353s ν(Pt-Cl). Raman: 2972w, 2923s, 2333s, 2308m, 1361w, 963w, 441w, 407w, 367w, 360w. m/z 349 (M$^+$).

4.9.2. [Pt(CH$_3$CN)$_4$](BF$_4$)$_2$

[PtCl$_2$(CH$_3$CN)$_2$] (1.73 g = 4.97 mmol) and $AgBF_4$ (1.94 g = 9.94 mmol) were suspended in CH_3CN (150 cm^3), the mixture refluxed for 4 h and filtered. The solution was reduced to a small volume on a rotary evaporator and the compound precipitated with Et_2O. The solid was filtered off, recrystallised from CH_3CN–Et_2O and dried in vacuo.

Yield: 2.51 g, 95%. Found: C, 18.0; H, 2.1; N, 10.3%. Calc. for $C_8H_{12}B_2F_8N_4Pt$: C, 18.0; H, 2.3; N, 10.5%. ^{1}H NMR (CD_3CN): δ 2.6 (t, ^4J(^{1}H, ^{195}Pt) 12 Hz). ^{13}C{^{1}H} NMR (CD_3CN): δ 3.8 (s). $\tilde{\nu}_{max}$ cm^{-1} 2918m (CH_3), 2338m ν(C≡N), 1061vs $\nu(BF_4^-)$, 533s, 521s. m/z 446 (M–BF$_4^-$).

4.10. Reaction of PNp$_x$Ph$_{3-x}$, PAnPh$_2$ and PAn$_2$Ph with [PtCl$_2$(COD)]

[PtCl$_2$(COD)] [7] (5 mg = 0.013 mmol) was dissolved in $CDCl_3$, a solution of the phosphine (0.027 mmol) in $CDCl_3$ added and a ^{31}P{^{1}H} NMR of the resulting clear solutions taken.

Table 8
Atomic coordinates and equivalent isotropic displacement coefficients ($Å^2$) for $[Au(PFc_2Ph)_2]PF_6 \cdot CHCl_3$

Atom	x	y	z	$U^a_{(eq)}$
Au	0.24688(7)	0.27308(3)	0.12383(9)	0.0412(5)
Fe(1)	0.4722(2)	0.2002(1)	−0.0464(3)	0.050(2)
Fe(2)	−0.0532(2)	0.1109(1)	−0.1013(3)	0.053(2)
Fe(3)	0.5202(2)	0.3768(1)	0.4581(3)	0.050(2)
Fe(4)	0.0082(2)	0.4007(1)	0.1625(3)	0.055(2)
P(1)	0.2451(4)	0.1747(2)	0.1002(5)	0.040(2)
P(2)	0.2878(4)	0.3733(2)	0.1583(5)	0.040(2)
C(1)	0.2279(8)	0.1424(4)	0.2505(10)	0.039(4)
C(2)	0.1523(8)	0.1630(4)	0.3193(10)	0.049(4)
C(3)	0.1319(8)	0.1364(4)	0.4297(10)	0.068(4)
C(4)	0.1869(8)	0.0892(4)	0.4713(10)	0.085(4)
C(5)	0.2625(8)	0.0687(4)	0.4025(10)	0.086(4)
C(6)	0.2830(8)	0.0953(4)	0.2921(10)	0.066(4)
C(7)	0.2761(7)	0.4054(4)	0.0012(9)	0.034(4)
C(8)	0.3416(7)	0.4611(4)	0.0032(9)	0.052(4)
C(9)	0.3245(7)	0.4864(4)	−0.1184(9)	0.055(4)
C(10)	0.2419(7)	0.4560(4)	−0.2419(9)	0.071(4)
C(11)	0.1764(7)	0.4002(4)	−0.2438(9)	0.065(4)
C(12)	0.1935(7)	0.3749(4)	−0.1223(9)	0.049(4)
C(111)	0.3893(7)	0.1645(4)	0.0852(8)	0.042(3)
C(112)	0.4098(7)	0.1201(4)	−0.0028(8)	0.050(3)
C(113)	0.5387(7)	0.1280(4)	0.0184(8)	0.063(3)
C(114)	0.5978(7)	0.1773(4)	0.1196(8)	0.070(3)
C(115)	0.5055(7)	0.1999(4)	0.1609(8)	0.041(3)
C(121)	0.3710(7)	0.2546(4)	−0.1585(8)	0.072(4)
C(122)	0.3721(7)	0.2055(4)	−0.2481(8)	0.100(4)
C(123)	0.4967(7)	0.2042(4)	−0.2376(8)	0.092(4)
C(124)	0.5728(7)	0.2525(4)	−0.1416(8)	0.070(4)
C(125)	0.4951(7)	0.2837(4)	−0.0927(8)	0.088(4)
C(211)	0.1315(6)	0.1283(4)	−0.0448(9)	0.042(3)
C(212)	0.0805(6)	0.1465(4)	−0.1752(9)	0.064(3)
C(213)	0.0079(6)	0.0966(4)	−0.2679(9)	0.079(3)
C(214)	0.0141(6)	0.0474(4)	−0.1947(9)	0.069(3)
C(215)	0.0905(6)	0.0671(4)	−0.0569(9)	0.057(3)
C(221)	−0.1161(6)	0.1673(4)	0.0202(9)	0.089(4)
C(222)	−0.1762(6)	0.1663(4)	−0.1228(9)	0.087(4)
C(223)	−0.2353(6)	0.1079(4)	−0.1790(9)	0.083(4)
C(224)	−0.2118(6)	0.0728(4)	−0.0707(9)	0.087(4)
C(225)	−0.1381(6)	0.1095(4)	0.0524(9)	0.094(4)
C(311)	0.4463(7)	0.3970(3)	0.2627(7)	0.042(3)
C(312)	0.5459(7)	0.3678(3)	0.2687(7)	0.055(3)
C(313)	0.6531(7)	0.4013(3)	0.3693(7)	0.057(3)
C(314)	0.6197(7)	0.4511(3)	0.4254(7)	0.050(3)
C(315)	0.4919(7)	0.4484(3)	0.3595(7)	0.051(3)
C(321)	0.3979(7)	0.3182(3)	0.5138(7)	0.073(4)
C(322)	0.5071(7)	0.2964(3)	0.5220(7)	0.093(4)
C(323)	0.6081(7)	0.3362(3)	0.6170(7)	0.089(4)
C(324)	0.5613(7)	0.3826(3)	0.6677(7)	0.095(4)
C(325)	0.4314(7)	0.3715(3)	0.6039(7)	0.089(4)
C(411)	0.1908(6)	0.4074(4)	0.2386(9)	0.042(3)
C(412)	0.1624(6)	0.4637(4)	0.2227(9)	0.074(3)
C(413)	0.0881(6)	0.4742(4)	0.3066(9)	0.073(3)
C(414)	0.0706(6)	0.4244(4)	0.3744(9)	0.075(3)
C(415)	0.1341(6)	0.3831(4)	0.3323(9)	0.063(3)
C(421)	−0.0648(6)	0.3353(4)	−0.0037(9)	0.078(4)
C(422)	−0.0785(6)	0.3899(4)	−0.0515(9)	0.094(4)
C(423)	−0.1476(6)	0.4168(4)	0.0201(9)	0.101(4)
C(424)	−0.1766(6)	0.3788(4)	0.1122(9)	0.085(4)
C(425)	−0.1254(6)	0.3284(4)	0.0974(9)	0.089(4)
P	0.9004(7)	0.2581(3)	0.5079(8)	0.100(3)
F(1)	0.9070(19)	0.1926(10)	0.5308(21)	0.086(3)
F(2)	0.9240(20)	0.3225(11)	0.4769(23)	0.133(4)

Table 8

Atom	x	y	z	$U_{(eq)}^{a}$
F(3)	0.9044(24)	0.2785(14)	0.6570(27)	0.136(4)
F(4)	1.0523(23)	0.2729(13)	0.5583(27)	0.136(4)
F(5)	0.8960(20)	0.2262(11)	0.3706(24)	0.258(4)
F(6)	0.7591(23)	0.2438(12)	0.4635(26)	0.162(4)
C	0.3324(22)	0.9405(12)	0.7007(24)	0.135(4)
Cl(1)	0.1990(14)	0.9472(6)	0.6326(16)	0.149(3)
Cl(2)	0.3758(11)	0.9172(5)	0.5498(14)	0.238(3)
Cl(3)	0.4711(16)	1.0059(8)	0.7326(19)	0.200(3)

[a] Equivalent isotropic U defined as one third of the trace of the orthogonalized U_{ij} tensor.

4.11. Reaction of PNp_xPh_{3-x}, $PAnPh_2$ and PAn_2Ph with $[PtCl_2(CH_3CN)]$

$[PtCl_2(CH_3CN)_2]$ (4.5 mg = 0.013 mmol) was dissolved in hot CH_3NO_2, a solution of the phosphine (0.027 mmol) in $CDCl_3$ added and a $^{31}P\{^1H\}$ NMR of the reaction mixture was taken. After two days, a precipitate had developed in samples containing $PNpPh_2$ and $PAnPh_2$, which was filtered off, washed with hexane and dried in vacuo.

4.11.1. Trans-$[PtCl_2(PNpPh_2)_2]$

Yield: 9.3 mg, 81%. Found: C,58.0; H,3.8%. Calc. for $C_{44}H_{34}Cl_2P_2Pt$: C, 59.3; H, 3.8%. $^{31}P\{^1H\}$ NMR ($CDCl_3$): δ 16.5 (t, $^1J(^{31}P, ^{195}Pt)$ 2600 Hz). ^1H NMR ($CDCl_3$): δ 9.1 (d, 1H), 7.9 (2d, 2H), 7.7 − 7.2 (m, 14H). $\tilde{\nu}_{max}$ cm^{-1} 344 m ν(Pt–Cl), bands characteristic for $PNpPh_2$.

4.11.2. Trans-$[PtCl_2(PAnPh_2)_2]$

Yield: 8.2 mg, 64%. Found: C, 63.1; H, 4.0%. Calc. for $C_{52}H_{38}Cl_2P_2Pt$: C, 63.0; H, 3.8%. $^{31}P\{^1H\}$ NMR ($CDCl_3$): δ 10.9 (t, $^1J(^{31}P, ^{195}Pt)$ 2584 Hz). ^1H NMR ($CDCl_3$): 8.6 (m), 8.0 (d), 7.6 (m), 7.4 − 7.1 (m). $\tilde{\nu}_{max}$ cm^{-1} 333m (Pt–Cl), bands characteristic for $PAnPh_2$.

4.12. Reaction of PNp_xPh_{3-x}, $PAnPh_2$ and PAn_2Ph with $[Pt(CH_3CN)_4](BF_4)_2$

$[Pt(CH_3CN)_4](BF_4)_2$ (7.1 mg = 0.013 mmol) was dissolved in hot CH_3CN, a solution of the phosphine (0.027 mmol) in $CDCl_3$ added and a $^{31}P\{^1H\}$ NMR of the reaction mixture was taken.

On a preparative scale the $[Pt(CH_3CN)_4](BF_4)2$ (0.100 g, 0.188 mmol) was dissolved in CH_3CN and a solution of the phosphine (0.376 mmol) in CH_2Cl_2 added. The mixture was filtered, the volume reduced and the compound precipitated with Et_2O. The product was filtered off, recrystallised from CH_2Cl_2–hexane and dried in vacuo.

4.12.1. Trans-$[Pt(CH_3CN)_2(PNpPh_2)_2](BF_4)_2$

Yield: 0.115 g, 57%. Found: C, 52.8; H, 3.8; N, 2.4%. Calc. for $C_{48}H_{40}B_2F_8N_2P_2Pt$: C, 53.6; H, 3.7; N, 2.6%. $^{31}P\{^1H\}$ NMR ($CDCl_3$): δ 13.3 (t, $^1J(^{31}P, ^{195}Pt)$ 2089 Hz). ^1H NMR (CD_3NO_2): δ 8.6 − 7.5 (m), 1.5 (s). $\tilde{\nu}_{max}$ cm^{-1} 3057m, 2927m $\nu(CH_3)$, 2336m ν(C≡N), 2314m ν(C≡N), 1060vs $\nu(BF_4^-)$, bands characteristic for $PNpPh_2$. m/z 988 ($M–BF_4^-$).

4.12.2. Trans-$[Pt(CH_3CN)_2(PNp_2Ph)_2](BF_4)_2$

Yield: 0.185 g, 84%. Found: C, 56.9; H, 4.0; N, 2.0%. Calc. for $C_{56}H_{44}B_2F_8N_2P_2Pt$: C, 57.2; H, 3.7; N, 2.4%. $^{31}P\{^1H\}$ NMR ($CDCl_3$): δ 10.7 (t, $^1J(^{31}P, ^{195}Pt)$ 2096 Hz). ^1H NMR (CD_3NO_2): δ 8.3 − 7.5 (m), 1.1 (b). $\tilde{\nu}_{max}$ cm^{-1} 3055s, 2923m $\nu(CH_3)$, 2335m ν(C≡N), 2316m ν(C≡N), 1068vs $\nu(BF_4^-)$, bands characteristic for PNp_2Ph. m/z 1088 ($M–BF_4^-$).

4.12.3. Trans-$[Pt(CH_3CN)_2(PNp_3)_2](BF_4)_2$

Yield: 0.176 g, 74%. Found: C, 57.4; H, 3.8; N, 2.1%. Calc. for one CH_2Cl_2 solvent molecule, $C_{65}H_{50}B_2Cl_2F_8N_2P_2Pt$: C, 57.4; H, 3.5; N, 2.1%. $^{31}P\{^1H\}$ NMR ($CDCl_3$): 11.2 (t, $^1J(^{31}P, ^{195}Pt)$ 2111 Hz). ^1H NMR (CD_3NO_2): δ 9.1 (b), 8.5 − 7.4 (m), 1.4 (s). $\tilde{\nu}_{max}$ cm^{-1} 2346m ν(C≡N), 2315m ν(C≡N), 1061vs $\nu(BF_4^-)$, bands characteristic for PNp_3. m/z 1019 (M-2 $CH_3CN–BF_4^–BF_4$).

4.12.4. Trans-[Pt(CH$_3$CN)$_2$(PAnPh$_2$)$_2$](BF$_4$)$_2$

Yield: 0.164 g, 74%. Found: C, 57.3; H, 3.9; N, 2.2%. Calc. for $C_{56}H_{44}B_2F_8N_2P_2Pt$: C, 57.2; H, 3.7; N, 2.4%. $^{31}P\{^1H\}$ NMR ($CDCl_3$): δ 1.5 (t, $^1J(^{31}P, ^{195}Pt)$ 2053 Hz). ^1H NMR (CD_3NO_2): δ 9.0 (s), 8.5 (d, $J(^1H, ^1H)$ 9 Hz), 8.2 (d, $J(^1H, ^1H)$ 9 Hz, 7.8 (m), 7.6 (m), 7.4 (m), 1.4 (s). $\tilde{\nu}_{max}$ cm^{-1} 3055s, 2926m $\nu(CH_3)$, 2334m $\nu(C\equiv N)$, 2313m $\nu(C\equiv N)$, 1061vs $\nu(BF_4^-)$, bands characteristic for $PAnPh_2$. *m/z* 1088 (M–BF_4^-).

4.12.5. Trans-[Pt(CH$_3$CN)$_2$(PAn$_2$Ph)$_2$](BF$_4$)$_2$

Yield: 0.175 g, 68%. Found: C, 59.5; H, 3.8; N, 2.1%. Calc. for one CH_2Cl_2 solvent molecule, $C_{73}H_{54}B_2Cl_2F_8N_2P_2Pt$: C, 60.0; H, 3.7; N, 1.9%. $^{31}P\{^1H\}$ NMR ($CDCl_3$): δ −2.9 (t, $^1J(^{31}P, ^{195}Pt)$ 2146 Hz). ^1H NMR (CD_3NO_2): δ 9.0 (s), 8.2 (d, $J(^1H, ^1H)$ 9 Hz), 8.0 (d, $J(^1H, ^1H)$ 9 Hz), 7.6 (m), 7.4 (m), 7.0 (m), 0.8 (b). $\tilde{\nu}_{max}$ cm^{-1} 3047s, 2925m $\nu(CH_3)$, 2335m $\nu(C\equiv N)$, 2314m $\nu(C\equiv N)$, 1060vs $\nu(BF_4^-)$, bands characteristic for PAn_2Ph. *m/z* 1288 (M-− BF_4^-).

Acknowledgements

BP is thanked for their generous endowment of D. M.P.M.'s chair. The EPSRC is thanked for funding C.M.M^{c}P. and T.M.W. and access to the CSD database at Daresbury. Dick Shepard and Paul Hammerton are thanked for running the resolution enhanced and two dimensional NMR spectra.

References

[1] D.M.P. Mingos, T.E. Muller, J. Organomet. Chem. 500 (1995) 251.
[2] J.P. Collman, L.S. Hegedus, J.R. Norton, R.G. Kinke, Principles and Applications of Organotransition Metal Chemistry, Mill Valley, CA, 1987, p. 67.
[3] F.H. Allen, J.E. Davies, J.J. Galloy, O. Johnson, O. Kennard, C.F. Marcae, E.M. Mitchell, G.F. Mitchell, J.M. Smith, D.G. Watson, J. Chem. Soc., Chem. Commun. 15 (1991) 1787, Cambridge structural database, 1993, Release 5.7, 126353 entries.
[4] T.E. Müller, S.W.K. Choi, D.M.P. Mingos, D. Murphy, D.J. Williams, V.W.W. Yam, J. Organomet. Chem. 484 (1984) 209.
[5] T.E. Müller, D.M.P. Mingos, D.J. Williams, J. Chem. Soc., Chem. Commun. 15 (1994) 1787.
[6] T.E. Müller, P.J. Barrie, C.J. Cardin, D.M.P. Mingos, C. Resende, J. Chem. Soc., Dalton Trans., 1997, submitted.
[7] T.E. Müller, F. Ingold, S. Menzer, D.M.P. Mingos, D.J. Williams, J. Organomet. Chem. 528 (1997) 163.
[8] J. Wesemann, P.G. Jones, D. Schomburg, L. Heuer, R. Schmutzler, Chem. Ber. 125 (1992) 2187.
[9] N.C. Baenziger, W.E. Bennett, D.M. Soborof, Acta Cryst. B 32 (1976) 962.
[10] K. Angermaier, E. Zeller, H. Schmidbaur, J. Organomet. Chem. 472 (1994) 371.
[11] C.S.W. Harker, E.R.T. Tiekink, Acta Cryst. C 46 (1990) 1546.
[12] P.G. Jones, C.F. Erdrügger, R. Hohbein, E. Schwarzmann, Acta Cryst. C 44 (1988) 1302.
[13] A. Houlton, R.M.G. Roberts, J. Silver, M.G.B. Drew, J. Chem. Soc., Dalton Trans., (1990) 1543.
[14] J.F. Nixon, A. Pidcok, in: E.F. Mooney (Ed.), Annual Review of NMP Spectroscopy, Academic Press, London, 2 (1969) 345.
[15] A.M. Saleem, H.A. Hodali, Inorg. Chim. Acta 174 (1990) 223.
[16] W. Henderson, R.D.W. Kemmit, C.J.S. Prouse, D.R. Russel, J. Chem. Soc., Dalton Trans., (1990) 1853.
[17] G.K. Anderson, H.C. Clark, J.A. Davies, G. Ferguson, M. Parvez, J. Cryst. Spect. Res. 12 (1982) 449.
[18] G.K. Anderson, H.K. Clark, J.A. Davies, Inorg. Chem. 20 (1981) 533.
[19] C.A. Tolman, Chem. Rev. 77 (1977) 31.
[20] B.J. Dunee, R.B. Morris, A.G. Orpen, J. Chem. Soc., Dalton Trans. (1991) 653.
[21] S.E. Garner, A.G. Orpen, J. Chem. Soc., Dalton Trans. (1993) 533.
[22] T.E. Müller, D.M.P. Mingos, Trans. Met. Chem., 20 (1995) 533.
[23] A.J. Gordon, R.A. Ford, The Chemist's Companion: A Handbook of Practical Data, Techniques and References, Wiley-Interscience, New York, 1972.
[24] G.M. Sheldrick, SHELXTL PC, Version 4.2, Siemens Analytical X-ray Instruments, Madison, WI, 1990.
[25] M.K. Cooper, P.A. Duckworth, K. Henrick, M. McPartlin, J. Chem. Soc., Dalton Trans. (1981) 2357.
[26] G.M. Sheldrick, SHELX-76, University of Cambridge, 1976.
[27] N. Walker, D. Stuart, Acta Cryst. A 39 (1983) 158.
[28] F.R. Hartley, S.G. Murray, C.A. McAuliffe, Inorg. Chem. 18 (1979) 1394.